

DNA Binding Studies of Pyridine-4-Carbohydrazone Derivatives: Molecular Docking, Chemical Synthesis and Spectroscopic Investigations

Sofian S. Mohamed¹, Salah M Bensaber², Nisreen H Meiqal², Amira A Gbaj², Anton Hermann³ and, Hamza S. Atiya⁴, Mohamed A. Ahmed⁴, Abdul M Gbaj^{2*}

¹Department of Chemistry and Toxins, Judicial Expertise and Research Center, Tripoli, Libya.

²Department of Medicinal Chemistry, Faculty of Pharmacy, University of Tripoli, Tripoli, Libya.

³Department of Biosciences, University of Salzburg, Salzburg, Austria.

⁴Department of Clinical Biochemistry, Faculty of Pharmacy, University of Tripoli, Tripoli, Libya.

***Corresponding Author:** Abdul M Gbaj, Professor of Genetics and Biochemistry, Department of Medicinal Chemistry, Faculty of Pharmacy, University of Tripoli, Tripoli, Libya. Tele: +218(0)214628098; Fax: +218(0)214625577; e-mail: ab.Gbaj@uot.edu.ly; P.O. Box 13645, Tripoli – Libya.

Citation: Mohamed SS, Bensaber SM, Meiqal NH, Hermann A, Atiya HS, et al. (2025) DNA Binding Studies of Pyridine-4-Carbohydrazone Derivatives: Molecular Docking, Chemical Synthesis and Spectroscopic Investigations. American J Cas Rep Rev: AJCRR-118.

Received Date: 10 March, 2025; **Accepted Date:** 24 March, 2025; **Published Date:** 31 March, 2025

Abstract

Introduction: DNA serves as a key target for drug development due to its structural accessibility, making it ideal for interaction with small molecules. The traditional drug discovery process is often slow and costly, prompting the need for more efficient approaches. In this study, we employed a combination of computational drug repositioning and molecular docking techniques to identify pyridine-4-carbohydrazone Schiff base derivatives with potential DNA-binding activity, expediting the identification of promising candidates for synthesis and experimental validation.

Methods: Nineteen pyridine-4-carbohydrazone Schiff base derivatives (INH01-INH19) were screened using molecular docking to predict their binding affinity to various DNA fragments. Compounds with the highest predicted affinities were synthesized using a microwave-assisted method and characterized via FTIR, ¹H, and ¹³C-NMR. The DNA-binding interactions of the synthesized compounds were further evaluated through UV-visible absorption titration and competitive binding assays with Rhodamine B to validate the computational predictions.

Results: Molecular docking identified key interactions between the derivatives and DNA, with aromatic planar structures and specific substitution patterns contributing to binding activity. Four lead compounds (INH03, INH09, INH14, and INH19) were synthesized and characterized. UV-visible absorption titration and competitive assays confirmed minor groove binding to genomic DNA. The binding constants (K_b) ranged from 6.3×10^4 - 7.4×10^4 M⁻¹, with negative Gibbs free energy values indicating spontaneous interactions.

Conclusion: This study identified four pyridine-4-carbohydrazone Schiff base derivatives with strong DNA-binding properties, underscoring their potential as DNA-targeting agents. The correlation between in silico predictions and experimental data demonstrates the utility of computational methods in guiding the design and development of DNA-interacting drugs.

Keywords: DNA-targeting drugs, Schiff base, Molecular docking, DNA binding studies.

1. Introduction

Deoxyribonucleic acid (DNA) is a fundamental macromolecule responsible for encoding genetic information and regulating various physiological processes (Hannon, 2007). It guides enzyme and protein synthesis through processes such as replication, transcription, and translation (Chatterjee et al., 2021; Saitou, 2018). Structurally, DNA is a double helix composed of two antiparallel polynucleotide strands, resembling a twisted ladder. These strands are stabilized primarily through Watson-Crick hydrogen bonds and form two parallel grooves: a major groove and a minor groove (Amshawee et al., 2024; Travers & Muskhelishvili, 2015). These grooves, differing in size and binding elements, provide distinct binding sites for small molecules and proteins (Laughlin-Toth et al., 2017; Zhitnikova & Shestopalova, 2017). DNA can adopt alternative conformations, influenced by environmental factors like hydration and ionic strength and can exist in forms such as A, B, C, D, and Z-form, with B-DNA being predominant in biological systems (Belmont et al., 2001).

More complex structures, including hairpin loops, triplexes (H-DNA), cruciform, and tetraplex, add to the structural diversity of DNA (Belmont et al., 2001; Biffi et al., 2013; Zeraati et al., 2018).

The study of DNA-small molecule interactions, including those involving drugs, organic dyes, and metal complexes, has gained considerable attention for its implications in understanding DNA's structural properties, elucidating drug mechanisms of action, and developing DNA-targeting therapies (Dayanidhi & Vaidyanathan, 2021; Lackner et al., 2024; Pandey & Adhikari, 2024; Yanthan & Bhattacharyya, 2023; Zhang et al., 2023). Due to DNA's well-defined three-dimensional structure and accessible functional groups, it has become a prime target in drug design (Alniss et al., 2024). Small molecules can interact with DNA primarily through two mechanisms: DNA cleavage or DNA binding. DNA binding interactions can be covalent or non-covalent (Silvestri & Brodbelt, 2013). Covalent interactions are typically irreversible, causing significant biological effects, while non-covalent interactions, such as intercalation, groove binding, and electrostatic interactions, are reversible and often less harmful (Ni et al., 2006).

Schiff bases, a class of compounds first synthesized by Hugo Schiff in 1864 (Tidwell, 2008), are of particular interest due to their broad biological activity and structural versatility (Biswas et al., 2024; Mushtaq et al., 2024). They are characterized by the azomethine group (-C=N-) and are typically formed by condensing primary amines with carbonyl compounds (Bedi et al., 2023; Hameed *et al.*, 2017). Their structural diversity and ease of synthesis, combined with their ability to coordinate with metals, make them valuable in medicinal chemistry (Catalano et al., 2021; Pour et al., 2019). Schiff bases are known for their antibacterial (Rollas et al., 2002; Yurttas *et al.*, 2013), antifungal (Karthikeyan et al., 2006; Pahontu et al., 2015), antiviral (Kaushik *et al.*, 2023; Pahontu et al., 2015)-anticancer (Iacopetta et al., 2021; Amim et al., 2016), anti-inflammatory (Biradar et al., 2021; Nithinchandra *et al.*, 2012; Pontiki et al., 2008), antimalarial (Sharma et al., 2014), antitubercular activities (Cordeiro & Kachroo, 2020; Ferreira *et al.*, 2009; Kumar et al., 2024; Amim et al., 2016), antidepressant (Mesripour et al., 2023; Sadia et al., 2021) and antihypertensive (Abdel-Wahab et al., 2008; Saadaoui et al., 2019). Additionally, they are precursors to a variety of bioactive heterocyclic compounds (Matsumoto et al., 2020), and are used in analytical applications (Hadjoudis & Mavridis, 2004), such as sensors (Chandran et al., 2024; Oiyee et al., 2019). SBs also have been extensively studied for their tribological activities, particularly their application as biolubricant additives (Kumar et al., 2019; Murmu et al., 2020). Furthermore, their use in catalyzing CO₂ fixation to mitigate atmospheric carbon accumulation has been well-documented (Ikiz et al., 2015; Kang et al., 2024; Yaseen et al., 2021).

In our previous work, we developed a series of pyridine-4-carbohydrazide Schiff base derivatives (INH01–INH19) by exploring the structural modification of pyridine-4-carbohydrazide as a core scaffold. Using computational tools, we predicted physicochemical properties, drug-likeness, bioactivity, PASS, and ADMET profiles, identifying compounds with promising attributes and reduced potential for adverse effects. This *in silico* approach enabled us to prioritize compounds for synthesis and screening based on their potential efficacy and safety profiles.

2. Materials and Methods

2.1. Molecular docking studies

Molecular docking is a computational approach to predict the binding orientation and interaction strength of small molecules (pyridine-4-carbohydrazide Schiff base derivatives) with biological targets (DNA) (Guedes et al., 2014; Rohs et al., 2005). The docking protocol was configured using AutoDock Vina in PyRx-Python Prescription 0.8, while Biovia Discovery Studio Visualizer was used to analyze the docking outcomes and visualize binding conformations.

The chemical structures of the compounds were generated using ChemDraw Ultra (see Table 1), and the 3D structures of selected

DNA fragments were sourced from the Protein Data Bank (<http://rcsb.org>) with PDB IDs: 1ZNA, 1D32, 1K2J, 1Z3F, 1MTG, 1ZEW, 3EYO, 102D, 1BNA, 2DNA, 330D, 181D, and 5MVK (see Table 2). Following download, the DNA structures were validated to ensure compatibility with docking protocols and alignment with experimentally reported DNA-ligand interactions. The docking study consisted of four primary steps: ligand preparation, DNA preparation, docking simulation, and post-docking analysis.

- **Ligand Preparation:** The ligands were prepared by optimizing their geometry to obtain the lowest energy conformation. This optimization was performed using density functional theory (DFT) calculations to minimize the energy of each compound. Subsequently, Gasteiger charges were assigned to the ligands, and non-polar hydrogen atoms were merged. The optimized structures were saved in Protein Data Bank (PDB) format for docking purposes.
- **DNA Preparation:** DNA fragments were prepared by removing unnecessary elements like water molecules, heteroatoms, and co-ligands from the crystal structures using Discovery Studio Visualizer. Polar hydrogen atoms were added to the DNA structure, and Kollman charges were assigned using AutoDock Tools. The finalized DNA structures were then saved in pdbqt format for the docking simulations.
- **Docking Process:** The docking process began with determining the coordinates and dimensions of the grid box, as summarized in Table 2, to define the search space for the docking simulations. The DNA fragments were treated as rigid molecules, while the ligands were treated flexible, allowing for conformational adjustments during the simulation. The docking simulations generated nine different ligand conformations for each DNA fragment, providing data on binding affinity (ΔG), RMSD upper bound, and RMSD lower bound. The conformation with the highest binding affinity and an RMSD value of zero for both the upper and lower bounds was considered the most favorable and was selected for further analysis. The selected ligand-DNA conformations were saved in Structure Data Format (SDF) for additional investigation.
- **Docking Analysis:** The ligand conformation with the highest binding affinity (ΔG) was subjected to detailed analysis using Discovery Studio Visualizer to examine DNA-ligand interactions. This analysis included the identification of hydrogen bonds, hydrophobic interactions, and other key interactions between the ligand and the DNA fragment. Graphs and visual representations of the docking interactions were plotted to facilitate a deeper understanding of the observed binding modes and molecular interactions.

Table 1: Codes and chemical structures of the designed compounds.

Codes	Chemical Structure	Codes	Chemical Structure
INH01		INH10	
INH02		INH11	
INH03		INH12	
INH04		INH13	
INH05		INH14	
INH06		INH15	
INH07		INH16	
INH08		INH17	
INH09		INH18	
INH19			

Table 2: Selected DNA Crystal Structures Utilized in Docking Studies.

DNA (PDB ID)	DNA forms	Number (bp)	Sequence	Centers of the Grid Box			Dimensions (Å) of the Grid Box		
				X	Y	Z	X	Y	Z
1D32	A form	4bp	d(CGCG) ₂	28.43 1	13.21 2	9.583	28.25 0	21.98 3	33.50 6
5MVK		12bp	d(CTACGCGCTAG) ₂	- 8.932	19.23 5	4.567	43.84 2	43.82 7	25.00
1K2J	B form	6bp	d(CGTCAG) ₂	- 0.906	2.442	8.121	28.22 3	25.83 6	26.54 8
1ZEW		10bp	d(CCTCTAGAGG) ₂	12.39 5	2.746	24.19 2	51.04 6	34.70 2	29.88 5
3EYO		10bp	d(ATATATATAT) ₂	17.03 6	12.16 9	87.99 5	47.46 8	34.25 7	50.93 2

330D		12bp	d(ACCGCCGGCGCC) ₂	- 7.747	18.83	- 1.898	57.68 7	44.60 2	37.77 9
102D		12bp	d(CGCAAATTTGCG) ₂	14.55 4	20.95 2	73.88	25.00	37.53 1	52.72
1BNA		12bp	d(CGCGAATTCGCG) ₂	14.77 8	21.51 8	8.804	30.79 9	31.88 4	25.00
2DNA		12bp	d(CGCGAATTCGCG) ₂	14.42 7	24.05 5	70.41 9	40.28 1	40.15 9	62.18 7
1MTG		6bp	d(GAGCTG) ₂	- 3.679	- 0.062 9	9.833	28.26 6	33.48 03	53.74 1
1Z3F		6bp	d(CGATCG) ₂	1.862	14.88 2	36.84 6	33.39 3	31.92 4	40.56 4
1ZNA	Z form	4bp	d(CGCG) ₂	8.796	18.01 8	- 8.299	25.00 0	25.00 0	25.00
181D		6bp	d(CACGCG) ₂	4.477	0.345	5.671	26.56 3	25.85 6	25.00

Abbreviations: Deoxyribonucleic acid (DNA); PDB ID (Protein Data Bank Identifier) is a unique code assigned to each structure within the Protein Data Bank (PDB); Base pair (bp); Nucleotide bases: adenine (A), cytosine (C), guanine (G), thymine (T). The grid box, where docking simulations occur, is defined along three axes: X (horizontal axis), Y (vertical axis), and Z (depth axis).

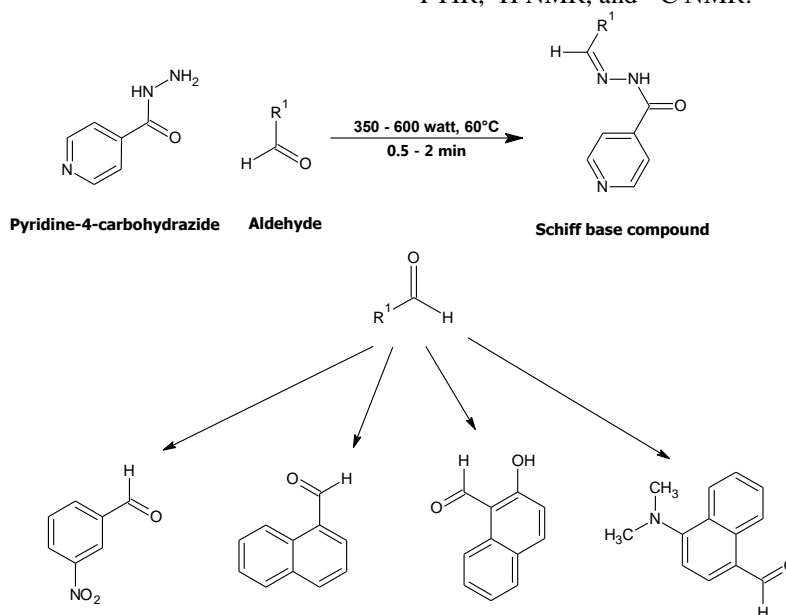
2.2. Chemical synthesis

All chemical reagents and solvents utilized in the synthesis of the target compounds were obtained from commercial suppliers and used without further purification. The reactions were conducted using microwave-assisted synthesis in a closed system (Milestone Start E, 2450 MHz, Italy), allowing for efficient reaction times and enhanced yields. Melting points were determined using an electrothermal apparatus (SMP30, Stuart, UK) with open glass capillary tubes, and the values were reported uncorrected (Cole-Parmer Ltd., Stone, UK).

Reaction progress and product purity were monitored by thin-layer chromatography (TLC) on 20 cm × 20cm aluminum sheets precoated with silica gel 60 F254 (0.20 mm layer thickness, Merck KGaA Analytical, Germany). Two mobile phases were employed: Phase 1 (chloroform:ethanol, 80:20) and Phase 2 (hexane:ethyl acetate, 30:70). TLC plates were visualized under UV light at 254 nm. Product yields were calculated based on the purified compounds.

Infrared (IR) spectra were recorded using a Fourier-transform infrared (FTIR) spectrometer (Cary-Varian 660, Australia) in the range of 4000–400cm⁻¹. Nuclear magnetic resonance (NMR) spectra were recorded on a Bruker Avance spectrometer operating at 400 MHz for ¹H NMR and 100 MHz for ¹³C NMR, with tetramethylsilane (TMS) as the internal standard. Deuterated dimethyl sulfoxide (DMSO-d₆) was used as the solvent, and chemical shifts (δ) were reported in ppm relative to the residual solvent peak. UV-visible absorption spectra were obtained at room temperature using a UV-visible spectrophotometer (Specord 200 Plus, UK), ensuring that relevant absorption maxima (λ_{max}) were recorded for each compound.

The synthesis of the target compounds (INH03, INH09, INH14, and INH19) followed the established synthetic protocol as detailed in our previous work (Alarabi et al., 2018). Reaction conditions are depicted in Scheme 1. The resulting crystalline products were dried thoroughly, and their structures were confirmed by comprehensive spectroscopic analyses, including FTIR, ¹H NMR, and ¹³C NMR.



Scheme 1: Synthesis pathway of the designed compounds.

2.3. Biological Evaluation

This section details the in-vitro investigation of DNA-binding interactions of synthesized compounds with human genomic DNA (G-DNA) using spectroscopic methods, specifically UV-visible absorption titration, and competitive fluorescence assays. These methods allow for the characterization of binding modes and the strength of interactions, which are vital in evaluating the potential of these compounds as DNA-targeted agents.

The genomic DNA used in these experiments was extracted from peripheral lymphocytes collected from anticoagulated blood (EDTA) samples, using a proteinase K digestion protocol followed by phenol/chloroform extraction (Ghatak et al., 2013). DNA purity was confirmed by measuring the absorbance ratio at 260 and 280 nm, which exceeded 1.9, indicating that the DNA was sufficiently free of protein contaminants (Marmur & Doty, 1962). The concentration of DNA per nucleotide was determined using absorption spectroscopy with a molar extinction coefficient of $6600 \text{ M}^{-1} \text{ cm}^{-1}$ at 260 nm (Rahman et al., 2017; Saha & Kumar, 2011). The stock solution was stored at 4°C in the dark for up to five days and regularly stirred to ensure homogeneity.

2.3.1. Study of DNA binding activity by UV-visible absorbance titration

UV-visible absorption spectroscopy is a critical tool for investigating the stability of DNA and its interactions with small ligand molecules (Ganeshpandian et al., 2014). Stock solutions of the synthesized compounds were prepared in a DMSO-Tris buffer mixture (1:9). During the titrations, the concentration of G-DNA was kept constant at $75 \mu\text{M}$, while the concentration of the test compounds was varied from 0 to $20 \mu\text{M}$. The total volume of each solution was adjusted to 2 mL using 0.01M Tris buffer (pH 7.4). After adding the compounds to the DNA solution, the mixtures were allowed to equilibrate for 8–10 minutes before gentle agitation. The absorption spectra were then recorded to observe potential shifts in absorbance, indicating interactions between the DNA and the ligands.

2.3.2. Study of DNA binding activity by competitive fluorescence assay

Fluorescence spectroscopy is a sensitive and widely used method for detecting interactions between DNA and small molecules. In this study, we employed a Jasco FP-6200 spectrofluorometer (Tokyo, Japan) to perform a competitive fluorescence assay using rhodamine B (RB) as a fluorescent probe. This assay was designed to evaluate the binding affinity of the synthesized compounds to G-DNA.

To prepare the DNA-RB complex, DNA was titrated with RB until a stable fluorescent complex was formed. The preformed DNA-RB complex was then titrated with increasing concentrations of the ligands (0– $30 \mu\text{M}$). Fluorescence measurements were taken after 30 minutes of equilibration at room temperature, allowing sufficient time for ligand-DNA interaction. The excitation wavelength was set at 550nm, and fluorescence emission was monitored at 577 nm over a spectral range of 560–650 nm. Both excitation and emission slit widths were maintained at 10.0 nm.

3. Results and discussion

3.1. Molecular docking studies

Molecular docking is the best alternative tool to rapidly predict binding conformations of ligands that are energetically favorable to interact with a pharmacological receptor site (de Ruyck et al., 2016; Torres et al., 2019). In addition, molecular docking provides information about the mechanism of binding of various molecules and drugs (Niazi & Mariam, 2024). It hence contributes significantly to designing new drugs and saving time and costs in the drug discovery and development pipeline (Kumar Shukla & Pradhan, 2024).

Molecular docking in this project was conducted to evaluate the DNA-binding modes, sequence selectivity, and preferred orientations of Schiff base derivatives of pyridine-4-carbohydrazide within various DNA fragments. Thirteen distinct DNA fragments, representing different conformations and base sequences, were utilized to model these interactions. The docking study aimed to explore how structural features of the compounds contribute to their DNA-binding behavior. Based on the structural similarities to known DNA-binding agents, two primary binding mechanisms were proposed: (i) intercalation, and (ii) groove binding.

To identify the DNA-binding mode more precisely, various crystal structures of DNA dodecamers were used, each possessing two long CG sequences and a long AT tract of base pairs, providing several potential binding sites. These specific sequences were selected to offer a detailed model for assessing how the Schiff base derivatives interact with different regions of the DNA, particularly focusing on whether intercalation or groove binding was the predominant mode of binding (Ricci & Netz, 2009).

In each docking experiment, the ligand conformation with the highest binding energy (ΔG) from nine potential conformations was selected for detailed analysis. The docking results revealed that several Schiff base derivatives displayed favorable DNA-binding affinities, with binding energies ranging from -5.7 to -9.1 kcal/mol, as summarized in Tables 3A and 3B.

Table 3A: Molecular Docking Results of the Designed Compounds with B-DNA Structures.

Codes	DNA Fragments (PDB ID)								
	B form								
	2DNA	1K2J	1ZEW	3EYO	330D	102D	1BNA	1MTG	1Z3F
INH01	-7.0	-7.1	-7.2	-6.7	-6.5	-7.0	-6.6	-5.6	-5.9
INH02	-7.2	-7.5	-7.5	-7.9	-6.8	-7.3	-6.8	-5.9	-6.0
INH03	-8.3	-8.4	-8.7	-8.6	-7.7	-8.5	-8.0	-6.6	-6.4
INH04	-7.2	-7.4	-7.4	-7.4	-6.5	-7.6	-7.1	-5.7	-5.4
INH05	-7.7	-7.6	-7.8	-7.8	-7.1	-7.8	-6.7	-6.4	-6.0
INH06	-7.7	-7.2	-7.9	-6.9	-7.1	-7.9	-6.8	-6.5	-6.4
INH07	-7.6	-7.6	-8.0	-7.8	-7.5	-7.8	-7.5	-6.3	-5.6
INH08	-7.4	-7.7	-7.5	-7.0	-7.0	-7.8	-6.7	-5.9	-5.8
INH09	-8.3	-8.6	-8.4	-7.7	-7.9	-8.4	-7.7	-6.7	-7.2
INH10	-7.9	-8.2	-8.3	-8.3	-7.9	-8.3	-7.2	-6.5	-6.1
INH11	-8.1	-8.2	-8.5	-8.8	-7.5	-8.4	-7.4	-6.3	-6.1
INH12	-8.1	-8.2	-8.4	-8.4	-8.0	-8.3	-7.4	-6.1	-6.1
INH13	-6.9	-7.1	-6.9	-6.5	-6.5	-7.0	-6.8	-5.4	-5.3
INH14	-8.7	-8.9	-8.9	-9.2	-7.9	-9.1	-8.8	-6.5	-6.5
INH15	-7.3	-7.4	-7.2	-6.9	-7.2	-7.3	-6.6	-5.7	-5.8
INH16	-6.7	-6.9	-6.4	-6.8	-6.0	-6.9	-6.6	-5.2	-5.0
INH17	-7.8	-7.2	-7.6	-7.7	-7.2	-8.1	-7.6	-6.2	-6.6
INH18	-7.5	-6.8	-7.7	-6.9	-6.8	-7.2	-6.9	-6.0	-6.0
INH19	-8.9	-8.6	-8.9	-8.8	-8.1	-9.0	-8.9	-6.5	-6.5
INH	-5.5	-5.4	-5.9	-5.6	-5.1	-5.8	-5.5	-4.6	-5.0
PT	-8.3	-6.3	-8.6	-6.3	-7.6	-8.4	-8.8	-6.9	-7.8

Abbreviations: INH=Isoniazid, PT=Paclitaxel. All Energy Values (ΔG) are Expressed in kcal/mol.

Table 3B: Molecular Docking Results of the Designed Compounds with A- and Z-DNA Structures.

Codes	DNA Fragments (PDB ID)			
	A form		Z form	
	1D32	5MVK	181D	1ZNA
INH01	-6.3	-6.2	-6.4	-5.7
INH02	-6.6	-6.5	-7.1	-6.3
INH03	-6.9	-6.8	-7.1	-6.7
INH04	-6.8	-6.1	-6.9	-6.2
INH05	-6.0	-6.8	-6.8	-6.3

INH06	-6.5	-6.5	-7.1	-6.2
INH07	-6.6	-6.7	-7.2	-6.1
INH08	-5.5	-6.3	-6.9	-5.9
INH09	-7.4	-7.3	-7.4	-6.5
INH10	-6.4	-6.9	-7.2	-6.7
INH11	-6.3	-7.0	-7.2	-6.8
INH12	-6.4	-6.7	-7.1	-6.7
INH13	-5.3	-5.7	-7.5	-6.3
INH14	-6.9	-7.4	-7.4	-7.1
INH15	-6.7	-6.4	-6.5	-5.9
INH16	-5.7	-6.4	-6.9	-5.8
INH17	-6.7	-7.1	-6.8	-6.3
INH18	-6.3	-6.3	-6.8	-6.1
INH19	-6.8	-7.2	-7.6	-6.8
INH	-5.4	-4.7	-5.0	-4.7
PT	-8.6	-10.5	-5.8	-6.6

Abbreviations: INH = Isoniazid, PT = Paclitaxel. All Energy Values (ΔG) are Expressed in kcal/mol.

More negative ΔG values suggest more stable ligand-DNA complexes, indicating strong geometric compatibility within the DNA helix (Laughton & Orozco, 2009; Pandey et al., 2020). Notably, derivatives INH14, INH19, INH09, and INH03 exhibited highly negative binding energies, with ΔG values approaching -9.0 kcal/mol, significantly outperforming the parent compound isoniazid (INH), which showed a lower binding affinity ($\Delta G = -5.4$ kcal/mol). The absence of aromatic substituents in INH limits its interactions with DNA to basic π - π stacking, unlike the more complex derivatives. In comparison to standard drugs paclitaxel (Taxol[®]), the INH derivatives generally demonstrated superior binding energies, particularly against B-form DNA, which was identified as the most favorable target, followed by Z-form and A-form DNA.

The results also underscore the significant influence of structural variations in pyridine-4-carbohydrazide derivatives on DNA-binding affinity and the stability of the resulting complexes. To explain how these structural differences impact binding efficacy, the derivatives were categorized based on the type of aromatic ring, the number of aromatic rings, and the presence of substituents (non-substituted, mono-substituted, or di-substituted). This categorization helped form a deeper understanding of the relationship between chemical structure and DNA-binding activity.

Moreover, the binding efficacy of the compounds was evaluated against the DNA fragment 1BNA, selected for its high-resolution crystal structure (1.90Å) and its common use in computational studies. Importantly, compounds that demonstrated strong binding to 1BNA also exhibited comparable binding activity with other DNA fragments. This indicates that structural modifications reducing binding efficacy against 1BNA would likely have a similar effect on other DNA fragments, highlighting the robustness of the structure-activity

relationship in predicting DNA-binding behavior across different targets.

The compounds incorporating two aromatic rings, particularly naphthalene-based derivatives such as INH09, INH14, and INH19, demonstrated significantly enhanced DNA-binding efficacy, with free energy changes (ΔG°) of -7.7, -8.8, and -8.9 kcal/mol, respectively. This superior performance contrasts with single aromatic ring compounds, such as phenyl-substituted derivatives (INH01, $\Delta G^\circ = -6.6$; INH18, $\Delta G^\circ = -6.9$), and heteroaromatic derivatives like furane (INH13, $\Delta G^\circ = -6.8$) and thiophene (INH16, $\Delta G^\circ = -6.6$). The enhanced binding efficiency of naphthalene-containing compounds is attributed to the increased π - π stacking interactions between the naphthalene moiety and DNA base pairs, reinforcing their capacity for stabilizing DNA-ligand complexes (Chen et al., 2018; Jourdan et al., 2012; Takenaka, 2017).

The DNA-binding activity of pyridine-4-carbohydrazide derivatives is significantly influenced by the presence of electron-donating groups (-OH, -OCH₃, -OCH₂CH₃, -CH₃, -N(CH₃)₂) and electron-withdrawing groups (-Cl, -NO₂) at various positions on the aromatic rings, which modulate DNA-binding affinity. Notably, the variations in binding efficacy observed among compounds such as INH01, INH03, INH12, and INH17 can be attributed to structural differences, particularly the presence and positional effects of nitro groups (-NO₂), as illustrated in Figure 1A. These groups alter the compounds' electronic properties and binding affinities by introducing additional hydrogen bonding and electrostatic interaction sites. Specifically, the meta-substituted nitro group in INH03 results in a modest increase in binding efficiency ($\Delta G^\circ = -8.0$ kcal/mol) compared to ortho (INH17, $\Delta G^\circ = -7.6$ kcal/mol) and para (INH12, $\Delta G^\circ = -7.4$ kcal/mol) substitution patterns. In contrast, the unsubstituted derivative INH01 exhibits lower binding activity ($\Delta G^\circ = -6.6$ kcal/mol). The

superior efficacy of INH03 is likely attributed to the optimal balance between electron-withdrawing effects and reduced steric hindrance at the meta position, facilitating enhanced hydrogen bonding and electrostatic interactions with negatively

charged DNA backbone (Colón et al., 2008; Jezuita et al., 2021; Szatylowicz et al., 2017). This underscores the pivotal role of nitro group positioning in modulating the DNA-binding properties of pyridine-4-carbohydrazone derivatives.

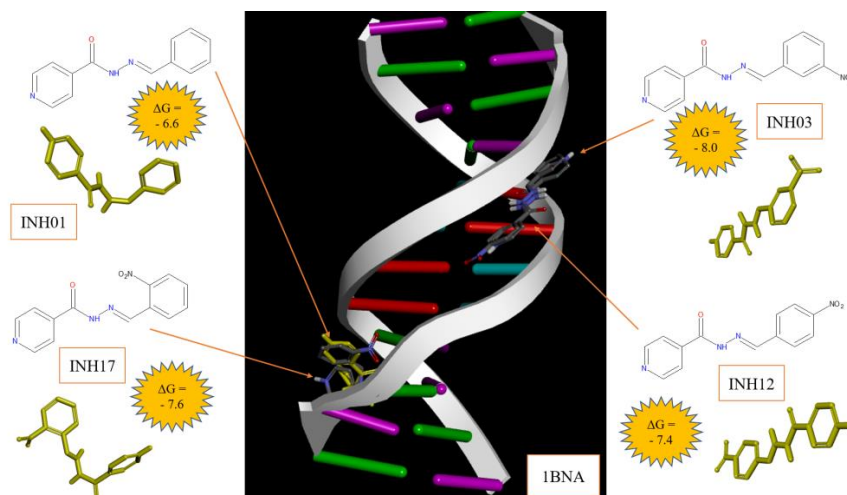


Figure 1A: Effect of the Nitro Group (NO₂) Position on the Localization of INH01, INH03, INH12, and INH17 within the Binding Site of 1BNA.

On the other hand, introducing electron-donating groups to the aromatic rings of mono-substituted pyridine-4-carbohydrazone derivatives generally result in reduced DNA-binding affinity, as indicated by the higher docking energies. This is observed in compounds such as INH02 (*o*-OH, $\Delta G^\circ = -6.8$), INH07 (*p*-N(CH₃)₂, $\Delta G^\circ = -7.5$), INH08 (*p*-OCH₃, $\Delta G^\circ = -6.7$), and INH09 (*o*-OH, $\Delta G^\circ = -7.7$) when compared to their non-substituted analogs INH01 ($\Delta G^\circ = -6.6$) and INH19 ($\Delta G^\circ = -9.0$). However, there are notable exceptions, particularly with INH14 (*p*-N(CH₃)₂, $\Delta G^\circ = -9.1$), which exhibits enhanced binding affinity. This can be attributed to the bulky nature of the dimethylamine group, which may facilitate stronger electrostatic interactions or engage in non-classical hydrogen bonding, thereby improving DNA binding.

The reduced binding affinity observed in INH09, despite the presence of an electron-donating hydroxyl group (-OH), can be explained by two key factors. First, the hydroxyl group at the 2-position of the naphthalene ring introduces steric hindrance, which disrupts optimal π - π stacking interactions between the naphthalene ring and DNA base pairs, weakening the binding (Ali et al., 2022). Second, although hydroxyl groups are typically favorable for hydrogen bonding, the positioning of the -OH group in INH09 limits its ability to form strong interactions with DNA. The planar and rigid structure of the naphthalene ring likely restricts the hydroxyl group's contribution to binding stabilization, diminishing its expected positive impact on DNA-binding affinity (Liu et al., 1996; Tanaka et al., 2010; Wei et al., 2014). An additional exception is observed in INH15, where the *p*-CH₃ group does not significantly alter binding energy compared to the non-substituted INH01 ($\Delta G^\circ = -6.6$). This is likely due to the weak electron-donating nature of the methyl

group and its limited ability to interact with DNA, resulting in similar binding behavior as seen in the unsubstituted derivative (Gil et al., 2016; Sánchez-González & Gil, 2021).

Furthermore, di-substituted derivatives, particularly those containing a balance of electron-donating and electron-withdrawing groups (e.g., INH10 and INH11, with $\Delta G^\circ = -7.2$ and -7.4 , respectively), demonstrate slightly superior binding affinity compared to their other di-substituted counterparts (INH05 ($\Delta G^\circ = -6.7$) and INH06 ($\Delta G^\circ = -6.8$)) as well as mono-substituted and non-substituted analogs. The enhanced binding activity of INH10 and INH11 can be attributed to the synergistic effects of electronic modulation, hydrogen bonding capabilities, and favorable π - π stacking interactions. The balanced combination of these substituents likely optimizes the molecular geometry and electronic distribution, leading to improved stabilization of the DNA-binding interactions.

Many of the pyridine-4-carbohydrazone Schiff base derivatives were found to predominantly bind in the DNA groove regions, with some exhibiting sequence-selective binding—preferentially aligning with either CG-rich or AT-rich regions within the minor grooves. For example, INH03 and INH09 bound within the same groove region, while INH01, INH14, and INH19 preferred a different groove as present in Figure 1B, further emphasizing the influence of aromatic ring types and substituents on binding site selection and affinity. Minor groove binders—such as these derivatives—are typically characterized by their flat, crescent shape, allowing for minimal steric hindrance (Lewis et al., 2011), and strong interactions in AT-rich regions, where the groove is narrower and deeper than in CG-rich regions (Hampshire & Fox, 2008; Pandya et al., 2010).

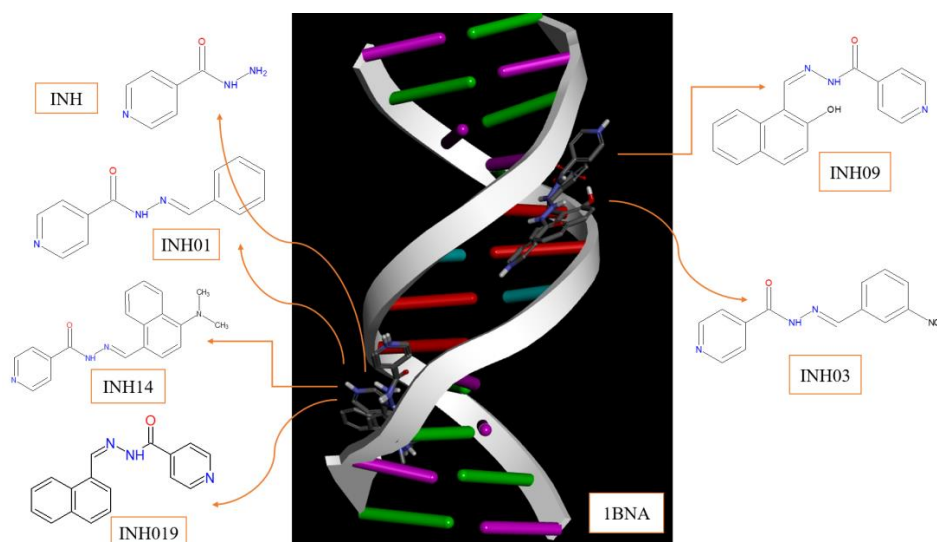


Figure 1B: Structure of the Complex between the DNA Dodecamer d(CGCGAATTCGCG)₂ and Chemical Compounds (INH01, INH03, INH09, INH14, INH19, and INH).

DNA minor groove binders are characterized by their flat crescent shape, the compounds exhibit multiple intermolecular forces, including hydrogen bonding, hydrophobic interactions, and electrostatic interactions, involving residues such as adenine (Ade), thymine (Thy), guanine (Gua), and cytosine (Cyt). Among these, hydrogen bonding and hydrophobic interactions contribute more significantly to the overall binding affinity. Furthermore, the R group (substituents) attached to the aromatic moiety facilitates intermolecular contact with DNA oligomers. Therefore, a comprehensive understanding of the general ethics governing predicted binding free energy provides valuable insight into the nature of various interactions contributing to molecular docking. Detailed information on ΔG values, base pairs located adjacent to the compounds on the binding sites, types, and number of binding interactions are available in Tables 4A-4I (refer to supplementary materials).

Finally, it can be inferred that the planar aromatic system and its substitution pattern significantly influence the activity of the different derivatives. Theoretical modeling experiments may aid in interpreting the binding of the compounds at the molecular level. This binding activity is attributed to a favorable structural environment, including an aryl group with a hydrophobic binding site, a hydrogen bonding domain (such as -CONH-group, -CH=N- group), an electron donor, an electron-withdrawing group, and another hydrophobic aryl ring in this hydrazone. Compounds INH03, INH09, INH14, and INH19 emerged as the most promising candidates for further chemical synthesis and biological screening, based on their strong binding affinities, superior docking scores compared to both INH and paclitaxel and favorable interactions with B-form DNA.

3.2. Chemical synthesis

In line with green chemistry principles, the synthetic reactions were designed to be environmentally friendly by minimizing hazardous reagents, reducing byproduct formation, and avoiding solvents wherever possible (Medina Valderrama et al., 2023; Rubab et al., 2022). A key technique employed in this study was microwave (MW) irradiation, which provides an efficient and sustainable alternative for both inorganic and organic synthesis. Compared to conventional thermal methods, MW irradiation offers higher yields and significantly shortens reaction times. This approach also contributes to pollution

prevention by minimizing the generation of harmful substances (Horikoshi & Serpone, 2019; Kappe, 2004).

In this study, pyridine-4-carbohydrazone was condensed with various substituted aldehydes under microwave irradiation, drastically reducing reaction times to between 0.5-2 minutes, while also simplifying workup procedures. By contrast, traditional synthesis of similar compounds typically requires 360-420 minutes under thermal conditions, often resulting in lower yields (Thomas et al., 2009). The synthesized compounds exhibited distinct and intense colors, which varied based on the electronic nature of the aldehyde substituent. Aldehydes with electron-donating groups were found to enhance reactivity and improve yields. The structures of the synthesized derivatives were confirmed using infrared (IR) spectroscopy, proton nuclear magnetic resonance (¹H-NMR), and carbon nuclear magnetic resonance (¹³C-NMR). The obtained spectral data matched the expected structures, validating the success of the synthesis.

N'-[(3-nitrophenyl)methylidene]pyridine-4-carbohydrazone [INH03]

The pure compound of **INH03** [M. F = C₁₃H₁₀N₄O₃, M. WT = 270.24] was recrystallized as a beige crystal from ethanol. % **Yield** = 90 %. **M.P** = 280-282 °C. **R_f**(chloroform: ethanol as solvent) = 0.60. **UV(DMSO)** λ_{max}: 345 nm. **FT-IR (cm⁻¹):** 3336.18 (NH-N), 3099.12 (C-H_{pyridine}), 3002.85 (C-H_{aromatic}), 1733.42 (C=O), 1639.35 (C=N), 1594.11 (asym, NO₂), 1557.23 (N-H_{bend}), 1547.39 (C=C_{aromatic}), 1363(sym, NO₂), 1144 (N-N). **¹H-NMR** (400MHz, DMSO-d₆): δ [ppm] 12.34 (s, 1H, NH-N), 8.82 (d, 2H, pyridine-H), 8.57 (s, 1H, HC=N), 7.86 (d, 2H, pyridine-H), 8.58 (d, 1H, aromatic-H), 8.30 – 8.19 (m, 2H, aromatic-H), 7.70 (d, 1H, aromatic-H). **¹³C-NMR** (100MHz, DMSO-d₆): δ [ppm] 162.37(C=O), 154.36(C=N), 150.52, 147.99(C=NO₂), 146.45, 140.26, 131.11, 128.18, 124.06, 121.55, 121.10.

(E)-N'-((2-hydroxynaphthalen-1-yl)methylene)pyridine-4-carbohydrazone [INH09]

The pure compound of **INH09** [M. F = C₁₇H₁₃N₃O₂, M. WT = 291.30] was recrystallized as a yellow crystal from ethanol. % **Yield** = 95.11 %. **M.P** = 270 – 272°C. **R_f**(chloroform: ethanol as solvent) = 0.73. **UV(DMSO)** λ_{max}: 368nm. **FT-IR (cm⁻¹):** 3360.73 (-OH), 3352.85 (N-H), 3160.12 (C-H_{aromatic}), 3043 (C-

H_{pyridine}, 1679.66 (C=O), 1626.21 (C=N), 1588.27 (C=C_{aromatic}), 1300.22 (C-O_{phenolic}). ¹H-NMR (400MHz, DMSO-d₆): δ [ppm] 12.53 (s, 1H, NH-N), 11.48 (s, 1H, OH), 8.85 (d, 2H, pyridine-H), 8.39 (s, 1H, HC=N), 7.90 (d, 2H, pyridine-H), 8.32–8.30 (d, 1H, Aromatic-H), 7.95–7.90 (m, 2H, aromatic-H), 7.64–7.60 (t, 1H, aromatic-H), 7.43–7.39 (t, 1H, aromatic-H), 7.26–7.23 (d, 1H, aromatic-H). ¹³C-NMR (100MHz, DMSO-d₆): δ [ppm] 161.19(C=O), 158.48, 151.27(C=N), 148.32, 146.19, 141.48, 132.92, 130.35, 128.85, 127.11, 123.89, 120.16, 119.04(C-OH), 117.18, 114.91, 109.38.

N'-((4-(dimethylamino) naphthalen-1-yl) methylene) pyridine-4-carbohydrazide [INH14]

The pure compound of **INH14** [M. F = C₁₉H₁₈N₄O, M.wt = 318.37] was recrystallized as a yellow crystal from ethanol. % **Yield** = 87.0 %. **M.P** = 220 – 222^oC. **R_f**(chloroform: ethanol as solvent) = 0.75. **UV**(DMSO) λ_{max}: 266, 375nm. **FT-IR**(cm⁻¹): 3323.19 (N-H str), 3112.35 (C-H_{aromatic} str), 2940.03 (C-H_{aliphatic} str), 1738.35 (amide II), 1727.93 (C=O str.), 1639.22 (C=N str.), 1576.00 (C=C_{aromatic}), 1310.12 (C-N str.), 836 (C-H_{bending}). ¹H-NMR (400 MHz, DMSO-d₆): δ [ppm] 12.10 (s, 1H, NH-N), 8.83 (d, 2H, pyridine-H), 8.68 (s, 1H, HC=N), 7.91 (d, 2H, pyridine-H), 7.91 - 7.26 (m, 6H, Aromatic-H), 3.47 (s, 6H, (CH₃)₂-N). ¹³C-NMR (100MHz, DMSO-d₆): δ [ppm] 161.28(C=O), 153.03, 150.32(C=N), 149.58, 144.95, 140.62, 131.67, 135.02, 131.67, 129.43, 124.82, 123.03, 122.81, 121.47, 113.22, 54.71(C-N-C).

N'-[(E)-(naphthalen-2-yl) methylenidene] pyridine-4-carbohydrazide [INH19]

The pure compound of **INH19** [M. F = C₁₇H₁₃N₃O, M. WT = 275.30] was recrystallized as a white crystal from ethanol. % **Yield** = 93.17 %. **M.P** = 177-179 °C. **R_f**(chloroform: ethanol as solvent) = 0.73. **UV**(DMSO) λ_{max}: 368nm. **FT-IR**(cm⁻¹): 3352.85 (NH-N), 1740.66 (C=O), 1646.21 (C=N), 1588.27 (C=C_{aromatic}). ¹H-NMR (400MHz, DMSO-d₆): δ [ppm] 12.18 (s, 1H, NH-N), 9.10 (s, 1H, HC=N), 8.85 (dd, 2H, pyridine-H), 8.05 (dd, 2H, pyridine-H), 7.98 -7.96 (m, 1H, aromatic-H), 7.90 (dd, 2H, aromatic-H), 7.72 – 7.61 (m, 3H, aromatic-H). ¹³C-NMR (100MHz, DMSO-d₆): δ [ppm] 161.55(C=O), 150.38(C=N), 148.99, 140.44, 133.53, 130.90, 130.19, 129.24, 128.83, 128.20, 127.45, 126.34, 125.57, 124.19, 121.51.

3.3. Biological Evaluation

This section evaluates the biological activity of the synthesized compounds, particularly their DNA-binding potential as suggested by molecular docking studies. The compounds INH03, INH09, INH14, and INH19 exhibited strong DNA-binding activity scores in silico, indicating significant interactions with DNA. Understanding the relationship between these compounds' molecular structures and their DNA-binding properties, including affinity and interactions, is essential to confirm their potential biological activity. Various methods exist to study DNA-small molecule interactions, with UV-visible and fluorescence spectroscopy being among the most widely used due to their simplicity, sensitivity, and reliability (Sirajuddin et al., 2013). These techniques allow for the monitoring of drug-DNA interactions by providing easily measurable optical properties that are sensitive to environmental changes. By offering qualitative and quantitative data, these methods complement each other and enable a comprehensive evaluation of drug-DNA binding, which is critical for drug development (Ni et al., 2006). The results from these experimental approaches will validate the molecular docking predictions and provide insights into the mechanisms of DNA-ligand interaction for the compounds in question. The compound INH14 was primarily used for the interpretation of experimental data related to binding activity. INH14 exhibited significant activity across all DNA fragments analyzed in the docking study.

3.3.1. UV-Visible absorption titration

UV-visible absorption spectrophotometry is a simple and effective technique for assessing interactions between small molecules and DNA (Khan et al., 2023). In this technique, changes in the absorption spectrum of free molecules and molecule-DNA complexes are monitored, or shifts in the spectrum of DNA are observed in the absence and presence of the compound. Various spectral changes (hypochromic, hyperchromic, bathochromic, and hypsochromic effects) provide information on the mode and extent of binding (Biver, 2012).

In this work, a fixed concentration of DNA was titrated with increasing amounts of the compound, and changes in the absorbance intensity and position of DNA's characteristic absorption band at 260 nm, corresponding to the π-π* transition of DNA base pairs, were recorded. The UV spectra of DNA, in the absence and presence of INH14, are illustrated in Figure 2A.

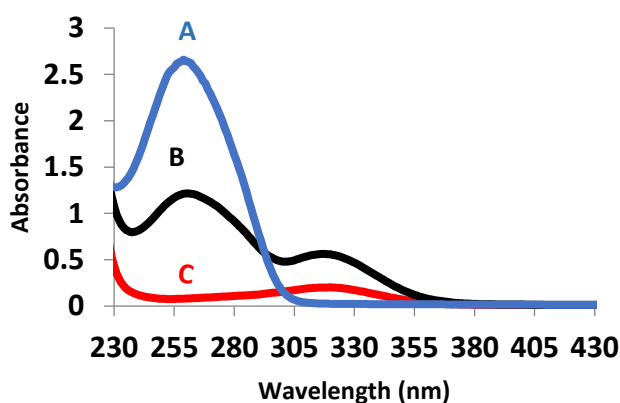


Figure 2: The UV absorption spectra of DNA in the absence and presence of an increasing concentration of INH14. (A) G-DNA alone, (B) G-DNA with 20μM INH014, and (C) INH014 alone.

The figure shows that the DNA's characteristic absorption peak at 260 nm (curve A) results from the base-conjugated double bonds in DNA. The compound INH014 exhibits two absorption peaks of varying intensity at 270 and 320 nm (curve C), likely due to $n-\pi^*$ electron transitions from the nitrogen in the hydrazone linkage and pyridine ring, along with $\pi-\pi^*$ electron transitions within the conjugated naphthalene and pyridine

systems. Upon interaction with DNA, the intensity of the 260 nm peak gradually decreases (hypochromic effect) with increasing compound concentration (curve B). This hypochromism indicates a contraction in the DNA helix axis and conformational changes in the DNA structure. However, no significant redshift was observed.

The percent hypochromic (% H) was calculated according to the following formula:

$$\% H = \frac{\epsilon_f - \epsilon_b}{\epsilon_f} \times 100$$

Where ϵ_f and ϵ_b are the absorbances of free and bound DNA, respectively.

Table 4. The percent hypochromic (% H), bathochromic shifts of synthesized compounds.

Codes	INH03	INH09	INH14	INH19
% H	1.38	1.41	1.41	1.39
Bathochromic shifts	1.11	1.18	1.21	1.18

The hypochromic effect (% H) and bathochromic shifts of the synthesized compounds INH03, INH09, INH14, and INH19 reveal a relationship between their structural features and binding properties, suggesting groove-binding interactions with DNA as presented in Table 4. The % H values, ranging modestly from 1.38 to 1.41, indicate minor reductions in absorption intensity upon binding. INH09 and INH14 exhibit the highest % H values (1.41), indicative of slightly stronger interactions or conformational changes. Similarly, the bathochromic shifts, ranging from 1.11 to 1.21nm, provide insights into electronic interactions. INH14, with the largest shift (1.21nm), benefits from the electron-donating dimethylamino group, enhancing conjugation and stabilizing the excited state, leading to stronger binding interactions. Conversely, INH03, featuring an electron-withdrawing nitro group, shows the smallest shift (1.11nm), likely due to reduced conjugation, while INH09's aromatic hydroxyl group facilitates $\pi-\pi$ stacking interactions.

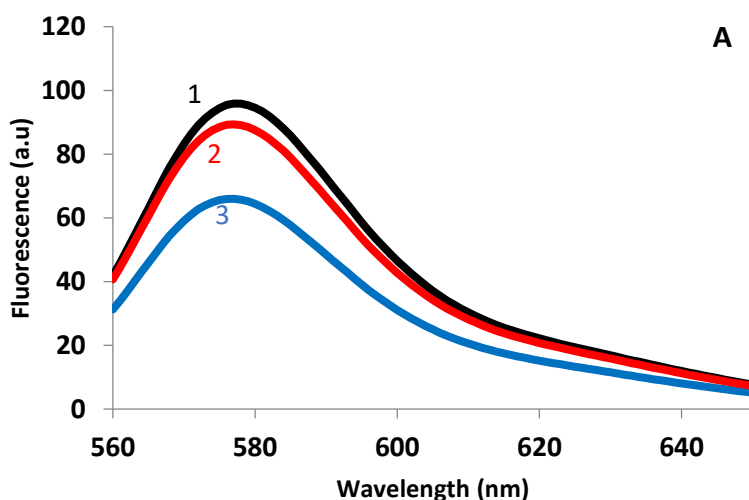
Despite these effects, the lack of significant changes in the UV absorption spectra suggests groove-binding as the primary interaction mode. Literature supports this hypothesis, as groove-binding molecules typically exhibit minimal hypochromic and bathochromic effects, with bathochromic shifts limited to 6–8nm (Rehman et al., 2015), unlike intercalation or covalent binding, which are characterized by substantial hypochromism (over 35%) and bathochromic shifts exceeding 15nm (Liu et al.,

2002; Sirajuddin, Ali, Haider, et al., 2012; Sirajuddin, Ali, Shah, et al., 2012). Covalent binding is also associated with hyperchromism and significant redshifts due to DNA structural disruption (Nakamoto et al., 2008), while electrostatic interactions induce hyperchromism, reflecting conformational changes (Arjmand & Jamsheera, 2011; Pratiel et al., 1998; Shahabadi et al., 2010). The modest spectral changes observed in these compounds strongly indicate groove-binding interactions, further supported by their structural features and substitution patterns.

To further confirm the groove-binding mode of these compounds, a competitive displacement assay was performed.

3.3.2. Competitive fluorescence assay

Fluorescence intensity changes often signal molecular interactions, making fluorescence spectroscopy a valuable tool for studying these interactions (Romani et al., 2010). However, the intrinsic fluorescence of DNA is weak, and the compounds studied here do not have fluorescent properties (Udenfriend & Zaltzman, 1962), making direct fluorescence measurement challenging. Rhodamine B (RB) was used as a fluorescent probe to overcome this. RB emits negligible fluorescence in aqueous solution (Fig. 3A, curve 3) but becomes highly fluorescent upon binding to the minor groove of DNA (Fig. 3A, curve 1), making it an ideal dye for studying DNA interactions (Yanthan & Bhattacharya, 2023).



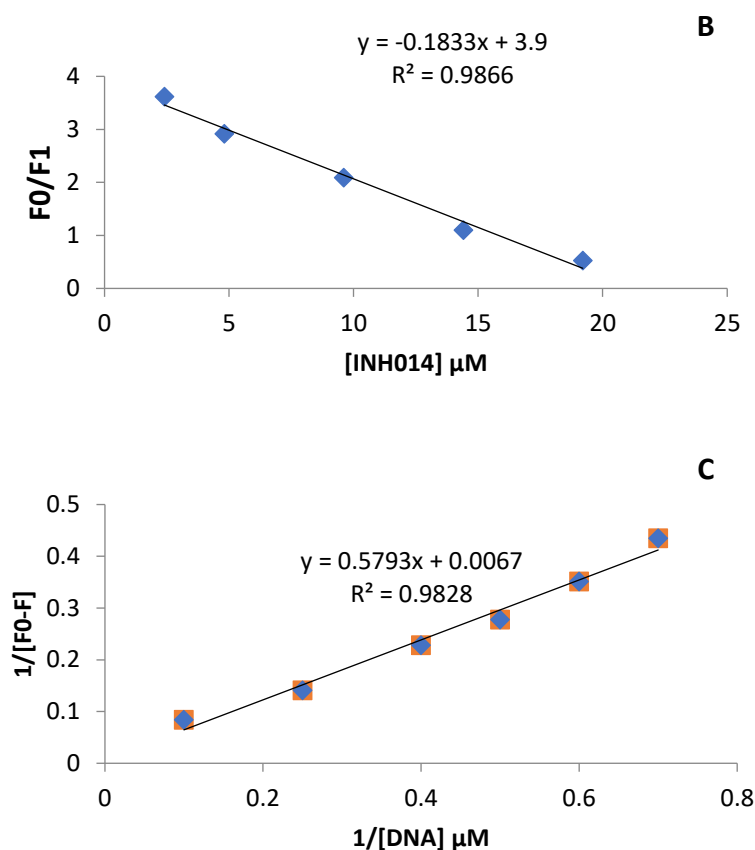


Fig. 3: (A) Interaction of INH14 with DNA using competitive displacement assays. Fluorescence emission spectra of DNA (50mM) in the presence of increasing concentrations of INH14 (15μM). The excitation wavelength was 550 nm. Spectra were recorded in the range of 562-650 nm. (B) Stern–Volmer plot for the quenching of fluorescence intensity of fluorescent RP-DNA systems by the successive addition of INH14 compound. (C) The binding constant (K_b) values were obtained from plots of plots of $1/(F_0-F)$ vs. $1/[DNA]$ at 298 K.

RB was chosen for its spectral-luminescence properties, which enable clear detection of changes in fluorescence emission upon binding with DNA. The binding behavior of RB is well understood, and when small molecules displace RB from its binding site, a quenching of fluorescence is observed, indicating interaction with the DNA. Figure 3A (Curve 2) shows the emission spectrum of the DNA-RB complex after the addition of INH14. As the concentration of INH14 increases, there is a notable decrease in fluorescence intensity, though the peak's position and shape remain unchanged. This quenching effect strongly suggests that INH14 displaces RB from its binding site on DNA.

Since the shape and position of the emission peak did not change, this indicates that INH14 does not intercalate between DNA base pairs but instead binds through a groove-binding mode. This conclusion is supported by the fact that intercalative binding would typically alter the spectral characteristics of the emission peak, which was not observed here. Therefore, the results confirm that INH14 and similar compounds bind to DNA through a non-intercalative, groove-binding mode.

To evaluate the fluorescence quenching efficiency, the Stern–Volmer quenching constant (K_{sv}) value was determined according to the following equation (Moodi et al., 2013):

$$(F_0/F) = 1 + K_{sv}[Q] \dots\dots\dots (1),$$

where F_0 and F are the fluorescence intensities before and after adding the quencher, respectively. $[Q]$ is the concentration of the quencher (compound). The slopes of the (F_0/F) vs. $[compound]$ plots yield the values of K_{sv} as presented in Fig. 3B and Table 5.

The binding constant (K_b) was determined using the Benesi–Hildebrand equation (Benesi & Hildebrand, 1949), which is commonly applied to evaluate the interaction strength between small molecules and macromolecules, such as DNA.

$$1 / (F_0 / F) = 1 / (F_0 / F) \times K_b + 1 / (F_0 / F) \dots\dots\dots (2)$$

where F_0 and F are the emission intensity of RB-DNA complex in the absence and presence of a quencher, respectively. K_b is the binding constant. From the plot of $1/(F_0-F)$ vs. $1/[DNA]$, K_b can be determined from the intercept and slope respectively (Fig. 3C and Table 5).

Using the value of the binding constant calculated above, the free energy of the interaction was calculated using the following relation:

$$\Delta G^\circ = - RT \ln K_b \dots\dots\dots (3),$$

where ΔG° is the observed binding free energy, which indicates the spontaneity/non-spontaneity of compound-DNA binding. R is the gas constant (8.314 J/mol/k or 1.987 cal/k mol), T is the absolute temperature (298.5 K), \ln is the natural logarithm, and K_b is the binding constant.

Table 5. The key selection vector (K_{SV}) values, binding constant (K_b), and free energy (ΔG) of synthesized compounds.

Codes	$K_{SV} (M^{-1})$	$K_b^1 (M^{-1})$	R^2 (5 points)	$\Delta G^\circ (Kcal\ mol^{-1})$
INH03	14.3×10^3	$6.3 \times 10^4 \pm 0.003$	0.968	-6.54
INH09	14.9×10^3	$6.5 \times 10^4 \pm 0.004$	0.978	-6.56
INH14	17.0×10^3	$7.4 \times 10^4 \pm 0.005$	0.99	-6.63
INH19	15.9×10^3	$7.3 \times 10^4 \pm 0.001$	0.98	-6.63
Paclitaxel	5.09×10^3	$5.3 \times 10^4 \pm 0.058$	0.99	-6.44
Daunorubicin	7.91×10^3	$7.2 \times 10^4 \pm 0.004$	0.97	-6.62

Abbreviations: 1 The mean value of three individual experiments with standard deviation (S.D.). 2 R is the correlation coefficient.

The data in Table 5 highlights the Key selection vector (K_{SV}) values, binding constants (K_b), and free energy changes (ΔG°) of the synthesized compounds (INH03, INH09, INH14, and INH19), demonstrating their affinity and interaction dynamics with DNA. The K_{SV} values indicate the ability of the compounds to displace Rhodamine B (RB) from DNA, reflecting their competitive binding to the RB-DNA complex. INH14 exhibited the highest K_{SV} value ($17.0 \times 10^3 M^{-1}$), surpassing other derivatives (INH19, INH09, and INH03) and the reference compounds paclitaxel and daunorubicin, indicating its superior ability to displace RB from DNA and its strongest binding to DNA among the synthesized compounds.

The binding constants (K_b), ranging from 6.3×10^4 to $7.4 \times 10^4 M^{-1}$, further underscore the robustness of the interactions. INH14, with the highest K_b ($7.4 \times 10^4 M^{-1}$), owes its strong binding affinity to the naphthalene moiety, which offers planar aromatic rings conducive to π - π stacking and hydrophobic interactions with DNA. Additionally, the presence of the dimethylamino group enhances electron density in the aromatic system, facilitating stronger electrostatic interactions with the negatively charged phosphate backbone of DNA. Conversely, INH03 exhibited the lowest K_b ($6.3 \times 10^4 M^{-1}$), likely due to the electron-withdrawing nitro group, which reduces electron density and weakens electrostatic and aromatic stacking interactions. INH09 and INH19 displayed intermediate to strong binding constants, attributed to their substituents enabling hydrogen bonding and π - π interactions.

The negative free energy values (ΔG°) for all compounds (-6.54 to -6.63 kcal/mol) confirm the spontaneity of the binding processes, with INH14 and INH19 sharing the most negative ΔG° values (-6.63 kcal/mol), indicating the most thermodynamically favorable interactions. This aligns with their strong binding constants and structural features that enhance interaction with DNA. Comparatively, paclitaxel displayed the lowest K_{SV} ($5.09 \times 10^3 M^{-1}$) and K_b ($5.3 \times 10^4 M^{-1}$) with a ΔG° of -6.44 kcal/mol, while daunorubicin showed higher K_b ($7.2 \times 10^4 M^{-1}$) and a ΔG° (-6.62 kcal/mol) close to those of INH14 and INH19, highlighting the superior binding affinity of the synthesized derivatives.

These trends in K_{SV} , K_b , and ΔG° are intricately tied to the electronic and steric properties of the substituents on the synthesized compounds. Electron-donating groups, such as the dimethylamino group in INH14, enhance conjugation and promote stronger π - π stacking and hydrophobic interactions, leading to higher binding affinity. In contrast, electron-

withdrawing groups like the nitro group in INH03 diminish these effects, weakening the interactions. The planar aromatic structures in INH09 and INH19, combined with their substituents, facilitate optimal stacking and van der Waals interactions, which are critical for binding efficiency. Collectively, these findings emphasize how structural modifications in the synthesized derivatives optimize their binding properties, offering valuable insights for the design of high-affinity DNA-binding agents.

4. Conclusion

This study provides detailed insights into the DNA-binding modes of several pyridine-4-carbohydrazide derivatives, which were designed based on previous work. Molecular docking results reveal a strong correlation with SAR analysis, highlighting the importance of planar aromaticity, substitution patterns, and functional groups (electron-donating/-withdrawing) in enhancing DNA-binding affinity. Hydrogen bonding and hydrophobic interactions, particularly between the planar aromatic moieties and the DNA backbone, emerged as key contributors to the overall binding affinity, especially in B-form DNA. Electrostatic interactions also play a role, further stabilizing the compound-DNA complex.

The compounds with the highest predicted affinities (INH03, INH09, INH14, INH19) were synthesized using a microwave-assisted method. This method proved efficient, providing high yields in significantly shorter reaction times compared to conventional synthesis techniques. Structural characterization through FTIR, 1H -NMR, and ^{13}C -NMR confirmed the successful synthesis of these derivatives. In-vitro binding studies confirmed that these compounds primarily bind to genomic DNA via minor groove binding. The binding constants (K_b) ranged from 6.3×10^4 to $7.4 \times 10^4 M^{-1}$, and the negative Gibbs free energy values confirmed the spontaneity and stability of these interactions.

Overall, this study emphasizes the utility of computational methods, particularly molecular docking and SAR analysis, in the early stages of drug discovery. The integration of computer-aided drug design (CADD) effectively streamlines the identification of promising DNA-binding agents by prioritizing compounds with high affinity, thereby reducing experimental costs and accelerating the development process. These findings set the stage for future research efforts aimed at designing optimized DNA-targeting compounds, contributing to advancements in therapeutic development and drug discovery.

References

1. Abdel-Wahab, B. F., Mohamed, S. F., Amr, A. E. G. E., & Abdalla, M. M. (2008). Synthesis and Reactions of Thiosemicarbazides, Triazoles, and Schiff Bases as Antihypertensive A-Blocking Agents. *Monatshefte Fur Chemie*, 139(9), 1083–1090. <https://doi.org/10.1007/S00706-008-0896-2>
2. Alarabi, H. I., Mohamed, S. S., Suayed, W. A., Al-Sadawe, I. A., Bensaber, S. M., Sherif, F. M., Hermann, A., & Gbaj, A. (2018). Antimicrobial Evaluation of Novel Metals Complexes Of N-Isonicotinamido-2-Hydroxy-5-Methoxybenzalaldimine. *Journal of Pharmacy and Pharmacology Research*, 2(2), 39–056. <https://doi.org/10.26502/Fjppr.0009>
3. Ali, I., Ahmed, B., Bezbaruah, M. J., Barukial, P., Upadhyaya, M., & Bezbaruah, B. (2022). DFT Study on The Conformational Change In π - π Stacking Interaction of Naphthalene, A-Naphthol and B-Naphthol Systems. *Rasayan Journal of Chemistry*, 15(2), 1190–1201. <https://doi.org/10.31788/Rjc.2022.1526929>
4. Alniss, H. Y., Al-Jubeh, H. M., Msallam, Y. A., Siddiqui, R., Makhlof, Z., Ravi, A., Hamdy, R., Soliman, S. S. M., & Khan, N. A. (2024). Structure-Based Drug Design of DNA Minor Groove Binders And Evaluation Of Their Antibacterial And Anticancer Properties. *European Journal of Medicinal Chemistry*, 271. <https://doi.org/10.1016/J.Ejmech.2024.116440>
5. Amshawee, A. M., Hussain, M. A., Muhtaser, S. T. M. Al, & Al-Faham, A. A. (2024). Structure, Functions and Clinical Significance Of Dna: A Review Article. *International Journal of Health & Medical Research*, 03(07). <https://doi.org/10.58806/Ijhm.2024.V3i07n07>
6. Arjmand, F., & Jamsheera, A. (2011). DNA Binding Studies Of New Valine Derived Chiral Complexes Of Tin(IV) And Zirconium(IV). *Spectrochimica Acta - Part A: Molecular and Biomolecular Spectroscopy*, 78(1), 45–51. <https://doi.org/10.1016/J.Saa.2010.06.009>
7. Bedi, P., Alanazi, A. K., Bose, R., & Pramanik, T. (2023). Recent Development of Synthetic Strategies Towards The Synthesis Of Azomethine Analogues: A Brief Review. In *Biointerface Research in Applied Chemistry* (Vol. 13, Issue 4). Amg Transcend Association. <https://doi.org/10.33263/Briac134.350>
8. Belmont, P., Constant, J. F., & Demeunynck, M. (2001). Nucleic Acid Conformation Diversity: From Structure to Function and Regulation. *Chemical Society Reviews*, 30(1), 70–81. <https://doi.org/10.1039/A904630e>
9. Benesi, H. A., & Hildebrand, J. H. (1949). Spectrophotometry Of Iodine with Aromatic Hydrocarbons 2703 [Contribution from The Chemical Laboratory of The University of California] A Spectrophotometric Investigation Of The Interaction Of Iodine With Aromatic Hydrocarbons.
10. Biffi, G., Tannahill, D., Mccafferty, J., & Balasubramanian, S. (2013). Quantitative Visualization Of Dna G-Quadruplex Structures In Human Cells. *Nature Chemistry*, 5(3), 182–186. <https://doi.org/10.1038/Nchem.1548>
11. Biradar, S. B., Narte, D. V., Kale, R. P., Momin, K. I., Sudewad, M. S., Tayade, K. C., & Palke, D. G. (2021). Synthesis, Spectral And Biological Studies Of Dha Schiff Bases. *Journal Of Applied Organometallic Chemistry*, 1(1), 41–47. <https://doi.org/10.22034/Jaoc.2021.275758.1003>
12. Biswas, T., Mittal, R. K., Sharma, V., Kanupriya, & Mishra, I. (2024). Schiff Bases: Versatile Mediators Of Medicinal And Multifunctional Advancements. In *Letters In Organic Chemistry* (Vol. 21, Issue 6, Pp. 505–519). Bentham Science Publishers. <https://doi.org/10.2174/0115701786278580231126034039>
13. Biver, T. (2012). Use Of Uv-Vis Spectrometry To Gain Information On The Mode Of Binding Of Small Molecules To DNAs And RNAs. In *Applied Spectroscopy Reviews* (Vol. 47, Issue 4, Pp. 272–325). <https://doi.org/10.1080/05704928.2011.641044>
14. Catalano, A., Sinicropi, M. S., Iacopetta, D., Ceramella, J., Mariconda, A., Rosano, C., Scali, E., Saturnino, C., & Longo, P. (2021). A Review On The Advancements In The Field Of Metal Complexes With Schiff Bases As Antiproliferative Agents. In *Applied Sciences (Switzerland)* (Vol. 11, Issue 13). Mdpi Ag. <https://doi.org/10.3390/App11136027>
15. Chandran, K. K., Thangaraj, B., Natesan Sundaramurthy, K., & Cingaram, R. (2024). A Schiff Base Colorimetric Sensor For Selective And Sensitive Detection Of Cr³⁺ Ions In Solution And Solid Matrix. *Materials Today Communications*, 40. <https://doi.org/10.1016/J.Mtcomm.2024.109768>
16. Chatterjee, S., Chauvier, A., Dandpat, S. S., Artsimovitch, I., & Walter, N. G. (2021). A Translational Riboswitch Coordinates Nascent Transcription-Translation Coupling. *Proceedings Of The National Academy Of Sciences Of The United States Of America*, 118(16). <https://doi.org/10.1073/Pnas.2023426118>
17. Chen, T., Li, M., & Liu, J. (2018). π - π Stacking Interaction: A Nondestructive And Facile Means In Material Engineering For Bioapplications. *Crystal Growth And Design*, 18(5), 2765–2783. <https://doi.org/10.1021/Acs.Cgd.7b01503>
18. Colón, I. G., González, F. A., Cordero, M., Zayas, B., Velez, C., Cox, O., Kumar, A., & Alegría, A. E. (2008). Role Of The Nitro Functionality In The DNA Binding Of 3-Nitro-10-Methylbenzothiazolo[3,2-A]Quinolinium Chloride. *Chemical Research In Toxicology*, 21(9), 1706–1715. <https://doi.org/10.1021/Tx800076c>
19. Cordeiro, R., & Kachroo, M. (2020). Synthesis And Biological Evaluation Of Anti-Tubercular Activity Of Schiff Bases Of 2-Amino Thiazoles. *Bioorganic And Medicinal Chemistry Letters*, 30(24). <https://doi.org/10.1016/J.Bmcl.2020.127655>
20. Dayanidhi, P. D., & Vaidyanathan, V. G. (2021). Structural Insights Into The Recognition Of DNA Defects By Small Molecules. In *Dalton Transactions* (Vol. 50, Issue 17, Pp. 5691–5712). Royal Society Of Chemistry. <https://doi.org/10.1039/D0dt04289g>
21. De Ruyck, J., Brysbaert, G., Blossey, R., & Lensink, M. F. (2016). Molecular Docking As A Popular Tool In Drug Design, An In Silico Travel. In *Advances And Applications In Bioinformatics And Chemistry* (Vol. 9, Issue 1). Dove Medical Press Ltd. <https://doi.org/10.2147/Aabc.S105289>
22. Ferreira, M. De L., Vasconcelos, T. R. A., De Carvalho, E. M., Lourenço, M. C. S., Wardell, S. M. S. V., Wardell, J. L., Ferreira, V. F., & De Souza, M. V. N. (2009). Synthesis And Antitubercular Activity Of Novel Schiff Bases Derived From D-Mannitol. *Carbohydrate Research*, 344(15), 2042–2047. <https://doi.org/10.1016/J.Carres.2009.08.006>
23. Ganeshpandian, M., Ramakrishnan, S., Palaniandavar, M., Suresh, E., Riyasdeen, A., & Akbarsha, M. A. (2014). Mixed Ligand Copper(Ii) Complexes Of 2,9-Dimethyl-

- 1,10-Phenanthroline: Tridentate 3n Primary Ligands Determine DNA Binding And Cleavage And Cytotoxicity. *Journal Of Inorganic Biochemistry*, 140, 202–212. <https://doi.org/10.1016/j.inorg.2014.10.021>
24. Ghatak, S., Mukherjee, R. B., & Nachimuthu, S. K. (2013). A Simple Method Of Genomic DNA Extraction From Human Samples For Pcr-Rflp Analysis. *Journal Of Biomolecular Techniques*, 24(4), 224–231. <https://doi.org/10.7171/jbt.13-2404-001>
25. Gil, A., Branchadell, V., & Calhorda, M. J. (2016). A Theoretical Study Of Methylation And Ch/π Interactions In DNA Intercalation: Methylated 1,10-Phenanthroline Adenine-Thymine Base Pairs. *Rsc Advances*, 6(89), 85891–85902. <https://doi.org/10.1039/C6ra15495f>
26. Guedes, I. A., De Magalhães, C. S., & Dardenne, L. E. (2014). Receptor-Ligand Molecular Docking. In *Biophysical Reviews* (Vol. 6, Issue 1, Pp. 75–87). <https://doi.org/10.1007/S12551-013-0130-2>
27. Hadjoudis, E., & Mavridis, I. M. (2004). Photochromism And Thermochromism Of Schiff Bases In The Solid State: Structural Aspects. *Chemical Society Reviews*, 33(9), 579–588. <https://doi.org/10.1039/B303644h>
28. Hameed, A., Al-Rashida, M., Uroos, M., Abid Ali, S., & Khan, K. M. (2017). Schiff Bases In Medicinal Chemistry: A Patent Review (2010-2015). In *Expert Opinion On Therapeutic Patents* (Vol. 27, Issue 1, Pp. 63–79). Taylor And Francis Ltd. <https://doi.org/10.1080/13543776.2017.1252752>
29. Hampshire, A. J., & Fox, K. R. (2008). The Effects Of Local DNA Sequence On The Interaction Of Ligands With Their Preferred Binding Sites. *Biochimie*, 90(7), 988–998. <https://doi.org/10.1016/j.biochi.2008.01.001>
30. Hannon, M. J. (2007). Supramolecular DNA Recognition. *Chemical Society Reviews*, 36(2), 280–295. <https://doi.org/10.1039/B606046n>
31. Horikoshi, S., & Serpone, N. (2019). Microwave Flow Chemistry As A Methodology In Organic Syntheses, Enzymatic Reactions, And Nanoparticle Syntheses. In *Chemical Record* (Vol. 19, Issue 1, Pp. 118–139). John Wiley And Sons Inc. <https://doi.org/10.1002/Tcr.201800062>
32. Iacopetta, D., Ceramella, J., Catalano, A., Saturnino, C., Bonomo, M. G., Franchini, C., & Sinicropi, M. S. (2021). Schiff Bases: Interesting Scaffolds With Promising Antitumoral Properties. In *Applied Sciences (Switzerland)* (Vol. 11, Issue 4, Pp. 1–20). Mdpi Ag. <https://doi.org/10.3390/App11041877>
33. Ikiz, M., Ispir, E., Aytar, E., Ulusoy, M., Karabuğa, Ş., Aslantaş, M., & Çelik, Ö. (2015). Chemical Fixation Of Co₂ Into Cyclic Carbonates By Azo-Containing Schiff Base Metal Complexes. *New Journal Of Chemistry*, 39(10), 7786–7796. <https://doi.org/10.1039/C5nj00571j>
34. Jezuita, A., Ejsmont, K., & Szatyłowicz, H. (2021). Substituent Effects Of Nitro Group In Cyclic Compounds. In *Structural Chemistry* (Vol. 32, Issue 1, Pp. 179–203). Springer. <https://doi.org/10.1007/S11224-020-01612-X>
35. Jourdan, M., Granzhan, A., Guillot, R., Dumy, P., & Teulade-Fichou, M. P. (2012). Double Threading Through DNA: Nmr Structural Study Of A Bis-Naphthalene Macrocyclic Bound To A Thymine-Thymine Mismatch. *Nucleic Acids Research*, 40(11), 5115–5128. <https://doi.org/10.1093/Nar/Gks067>
36. Kang, N., Fan, Y., Li, D., Jia, X., & Zhao, S. (2024). Preparation Of Magnetic Nano-Catalyst Containing Schiff Base Unit And Its Application In The Chemical Fixation Of Co₂ Into Cyclic Carbonates. *Magnetochemistry*, 10(5). <https://doi.org/10.3390/Magnetochemistry10050033>
37. Kappe, C. O. (2004). Controlled Microwave Heating In Modern Organic Synthesis. In *Angewandte Chemie - International Edition* (Vol. 43, Issue 46, Pp. 6250–6284). <https://doi.org/10.1002/Anie.200400655>
38. Karthikeyan, M. S., Prasad, D. J., Poojary, B., Subrahmanya Bhat, K., Holla, B. S., & Kumari, N. S. (2006). Synthesis And Biological Activity Of Schiff And Mannich Bases Bearing 2,4-Dichloro-5-Fluorophenyl Moiety. *Bioorganic And Medicinal Chemistry*, 14(22), 7482–7489. <https://doi.org/10.1016/J.Bmc.2006.07.015>
39. Kaushik, S., Paliwal, S. K., Iyer, M. R., & Patil, V. M. (2023). Promising Schiff Bases In Antiviral Drug Design And Discovery. In *Medicinal Chemistry Research* (Vol. 32, Issue 6, Pp. 1063–1076). Springer. <https://doi.org/10.1007/S00044-023-03068-0>
40. Khan, S., Rahman, F. U., Zahoor, M., Haq, A. U., Shah, A. B., Rahman, M. U., & Rahman, H. U. (2023). The Dna Threat Probing Of Some Chromophores Using Uv/Vis Spectroscopy. *World Journal Of Biology And Biotechnology*, 8(2), 19. <https://doi.org/10.33865/Wjb.008.02.0962>
41. Kumar, B., Devi, J., Dubey, A., & Kumar, M. (2024). Biological And Computational Studies Of Hydrazone Based Transition Metal(Ii) Complexes. *Chemistry & Biodiversity*. <https://doi.org/10.1002/Cbdv.202401116>
42. Kumar, B., Kuntail, J., Verma, D. K., Rastogi, R. B., & Sinha, I. (2019). Mechanism Of Triboactivity Of Schiff Bases: Experimental And Molecular Dynamics Simulations Studies. *Journal Of Molecular Liquids*, 289. <https://doi.org/10.1016/J.Molliq.2019.111171>
43. Kumar Shukla, A., & Pradhan, J. (2024). Applications Of Molecular Docking Techniques In Repurposing Of Drug. In *Unravelling Molecular Docking - From Theory To Practice* [Working Title]. Intechopen. <https://doi.org/10.5772/Intechopen.1004703>
44. Lackner, A., Qiu, Y., Armanus, E., Macapagal, A. N. K., Leonidas, L., Xu, H., & McNulty, R. (2024). Measuring Interactions Between Proteins And Small Molecules Or Nucleic Acids. *Current Protocols*, 4(7). <https://doi.org/10.1002/Cpz1.1105>
45. Laughlin-Toth, S., Carter, E. K., Ivanov, I., & Wilson, W. D. (2017). DNA Microstructure Influences Selective Binding Of Small Molecules Designed To Target Mixed-Site DNA Sequences. *Nucleic Acids Research*, 45(3), 1297–1306. <https://doi.org/10.1093/Nar/Gkw1232>
46. Loughton, C. A., & Orozco, M. (2009). Nucleic Acid Simulations Themed Issue. In *Physical Chemistry Chemical Physics* (Vol. 11, Issue 45, Pp. 10541–10542). <https://doi.org/10.1039/B921472k>
47. Lewis, E. A., Munde, M., Wang, S., Rettig, M., Le, V., Machha, V., & Wilson, W. D. (2011). Complexity In The Binding Of Minor Groove Agents: Netropsin Has Two Thermodynamically Different DNA Binding Modes At A Single Site. *Nucleic Acids Research*, 39(22), 9649–9658. <https://doi.org/10.1093/Nar/Gkr699>
48. Liu, J., Zhang, T., Lu, T., Qu, L., Zhou, H., Zhang, Q., & Ji, L. (2002). D Na-Binding And Cleavage Studies Of Macrocyclic Copper(Ii) Complexes. In *Journal Of Inorganic Biochemistry* (Vol. 91). www.Elsevier.Com/Locate/Jinorgbio

49. Liu, Z. R., Hecker, K. H., & Rill, R. L. (1996). Selective DNA Binding Of (N-Alkylamine)-Substituted Naphthalene Imides AndDiimides To G+C-Rich DNA. *Journal Of Biomolecular Structure And Dynamics*, 14(3), 331–339. <https://doi.org/10.1080/07391102.1996.10508128>
50. Marmur, J., & Doty, P. (1962). Determination Of The Base Composition Of Deoxyribonucleic Acid From Its Thermal Denaturation Temperature. *Journal Of Molecular Biology*, 5(1), 109–118. [https://doi.org/10.1016/S0022-2836\(62\)80066-7](https://doi.org/10.1016/S0022-2836(62)80066-7)
51. Matsumoto, Y., Sawamura, J., Murata, Y., Nishikata, T., Yazaki, R., & Ohshima, T. (2020). Amino Acid Schiff Base Bearing Benzophenone Imine As A Platform For Highly Congested Unnatural α -Amino Acid Synthesis. *Journal Of The American Chemical Society*, 142(18), 8498–8505. <https://doi.org/10.1021/jacs.0c02707>
52. Medina Valderrama, C. J., Morales Huamán, H. I., Valencia-Arias, A., Vasquez Coronado, M. H., Cardona-Acevedo, S., & Delgado-Caramutti, J. (2023). Trends In Green Chemistry Research Between 2012 And 2022: Current Trends And Research Agenda. *Sustainability (Switzerland)*, 15(18). <https://doi.org/10.3390/Su151813946>
53. Mesripour, A., Jafari, E., Hajibeiki, M. R., & Hassanzadeh, F. (2023). Design, Synthesis, Docking, And Antidepressant Activity Evaluation Of Isatin Derivatives Bearing Schiff Bases. *Iranian Journal Of Basic Medical Sciences*, 26(4), 438–444. <https://doi.org/10.22038/Ijbm.2023.68363.14916>
54. Moodi, A., Khorasani-Motlagh, M., Noroozifar, M., & Niroomand, S. (2013). Binding Analysis Of Ytterbium(III) Complex Containing 1,10-Phenanthroline With DNA And Its Antimicrobial Activity. *Journal Of Biomolecular Structure And Dynamics*, 31(8), 937–950. <https://doi.org/10.1080/07391102.2012.718525>
55. Murmu, M., Sengupta, S., Pal, R., Mandal, S., Murmu, N. C., & Banerjee, P. (2020). Efficient Tribological Properties Of Azomethine-Functionalized Chitosan As A Bio-Lubricant Additive In Paraffin Oil: Experimental And Theoretical Analysis. *Rsc Advances*, 10(55), 33401–33416. <https://doi.org/10.1039/D0ra07011d>
56. Mushtaq, I., Ahmad, M., Saleem, M., & Ahmed, A. (2024). Pharmaceutical Significance Of Schiff Bases: An Overview. *Future Journal Of Pharmaceutical Sciences*, 10(1). <https://doi.org/10.1186/S43094-024-00594-5>
57. Nakamoto, Kazuo., Tsuboi, Masamichi., & Strahan, G. D. (2008). *Drug-Dna Interactions: Structures And Spectra*. John Wiley & Sons.
58. Ni, Y., Lin, D., & Kokot, S. (2006). Synchronous Fluorescence, Uv-Visible Spectrophotometric, And Voltammetric Studies Of The Competitive Interaction Of Bis(1,10-Phenanthroline)Copper(II) Complex And Neutral Red With DNA. *Analytical Biochemistry*, 352(2), 231–242. <https://doi.org/10.1016/J.Ab.2006.02.031>
59. Niazi, S. K., & Mariam, Z. (2024). Computer-Aided Drug Design And Drug Discovery: A Prospective Analysis. In *Pharmaceuticals* (Vol. 17, Issue 1). Multidisciplinary Digital Publishing Institute (Mdpi). <https://doi.org/10.3390/Ph17010022>
60. Nithinchandra, Kalluraya, B., Aamir, S., & Shabaraya, A. R. (2012). Regioselective Reaction: Synthesis, Characterization And Pharmacological Activity Of Some New Mannich And Schiff Bases Containing Sydnone. *European Journal Of Medicinal Chemistry*, 54, 597–604. <https://doi.org/10.1016/J.Ejmech.2012.06.011>
61. Oiyé, É. N., Ribeiro, M. F. M., Katayama, J. M. T., Tadini, M. C., Balbino, M. A., Eleotério, I. C., Magalhães, J., Castro, A. S., Silva, R. S. M., Da Cruz Júnior, J. W., Dockal, E. R., & De Oliveira, M. F. (2019). Electrochemical Sensors Containing Schiff Bases And Their Transition Metal Complexes To Detect Analytes Of Forensic, Pharmaceutical And Environmental Interest. A Review. In *Critical Reviews In Analytical Chemistry* (Vol. 49, Issue 6, Pp. 488–509). Taylor And Francis Ltd. <https://doi.org/10.1080/10408347.2018.1561242>
62. Pahontu, E., Julea, F., Rosu, T., Purcarea, V., Chumakov, Y., Petrenco, P., & Gulea, A. (2015). Antibacterial, Antifungal And In Vitro Antileukaemia Activity Of Metal Complexes With Thiosemicarbazones. *Journal Of Cellular And Molecular Medicine*, 19(4), 865–878. <https://doi.org/10.1111/Jcmm.12508>
63. Pandey, A., & Adhikari, A. (2024). Free Energy Calculations Reveal The Interaction And Stability Of Ligands In The Vicinity Of B-DNA Dodecamer. *Main Group Chemistry*, 23(1), 89–102. <https://doi.org/10.3233/Mgc-230031>
64. Pandey, A., Upadhyaya, A., Kumar, S., & Yadav, A. K. (2020). Interaction, Dynamics And Stability Analysis Of Some Minor Groove Binders With B-DNA Dodecamer 5'-(CGCAATTGCG)-3'. *Drug Des. In Drug Des* (Vol. 10, Issue 1).
65. Pandya, P., Islam, M., Suresh Kumar, G., Jayaram, B., & Kumar, S. (2010). DNA Minor Groove Binding Of Small Molecules: Experimental And Computational Evidence. In *J. Chem. Sci* (Vol. 122, Issue 2).
66. Pontiki, E., Hadjipavlou-Litina, D., & Chaviara, A. T. (2008). Evaluation Of Anti-Inflammatory And Antioxidant Activities Of Copper (II) Schiff Mono-Base And Copper(II) Schiff Base Coordination Compounds Of Dien With Heterocyclic Aldehydes And 2-Amino-5-Methyl-Thiazole. *Journal Of Enzyme Inhibition And Medicinal Chemistry*, 23(6), 1011–1017. <https://doi.org/10.1080/14756360701841251>
67. Pour, S. R., Abdolmaleki, A., & Dinari, M. (2019). Immobilization Of New Macrocyclic Schiff Base Copper Complex On Graphene Oxide Nanosheets And Its Catalytic Activity For Olefins Epoxidation. *Journal Of Materials Science*, 54(4), 2885–2896. <https://doi.org/10.1007/S10853-018-3035-4>
68. Pratiel, G., Bernadou, J., & Meunier, B. (1998). DNA And Rna Cleavage By Metal Complexes. In *Advances In Inorganic Chemistry* (Vol. 45).
69. Rahman, Y., Afrin, S., Husain, M. A., Sarwar, T., Ali, A., Shamsuzzaman, & Tabish, M. (2017). Unravelling The Interaction Of Pirenzepine, A Gastrointestinal Disorder Drug, With Calf Thymus DNA: An In Vitro And Molecular Modelling Study. *Archives Of Biochemistry And Biophysics*, 625–626, 1–12. <https://doi.org/10.1016/J.Abb.2017.05.014>
70. Rehman, S. U., Sarwar, T., Husain, M. A., Ishqi, H. M., & Tabish, M. (2015). Studying Non-Covalent Drug-DNA Interactions. In *Archives Of Biochemistry And Biophysics* (Vol. 576, Pp. 49–60). Academic Press Inc. <https://doi.org/10.1016/J.Abb.2015.03.024>
71. Ricci, C. G., & Netz, P. A. (2009). Docking Studies On DNA-Ligand Interactions: Building And Application

- Chemical Information And Modeling, 49(8), 1925–1935. <https://doi.org/10.1021/Ci9001537>
72. Rohs, R., Bloch, I., Sklenar, H., & Shakked, Z. (2005). Molecular Flexibility In Ab Initio Drug Docking To DNA: Binding-Site And Binding-Mode Transitions In All-Atom Monte Carlo Simulations. *Nucleic Acids Research*, 33(22), 7048–7057. <https://doi.org/10.1093/Nar/Gki1008>
73. Rollas, S., Gulerman, N., & Erdeniz, H. (2002). Synthesis And Antimicrobial Activity Of Some New Hydrazones Of 4-Fluorobenzoic Acid Hydrazide And 3-Acetyl-2,5-Disubstituted-1,3,4-Oxadiazolines. In *Il Farmaco* (Vol. 57). www.elsevier.com/locate/farmac
74. Romani, A., Clementi, C., Miliani, C., & Favaro, G. (2010). Fluorescence Spectroscopy: A Powerful Technique For The Noninvasive Characterization Of Artwork. *Accounts Of Chemical Research*, 43(6), 837–846. <https://doi.org/10.1021/Ar900291y>
75. Rubab, L., Anum, A., Al-Hussain, S. A., Irfan, A., Ahmad, S., Ullah, S., Al-Mutairi, A. A., & Zaki, M. E. A. (2022). Green Chemistry In Organic Synthesis: Recent Update On Green Catalytic Approaches In Synthesis Of 1,2,4-Thiadiazoles. In *Catalysts* (Vol. 12, Issue 11). [Mdpi. https://doi.org/10.3390/Catal12111329](https://doi.org/10.3390/Catal12111329)
76. S. Amim, R., Pessoa, C., C. S. Lourenco, M., V. N. De Souza, M., & A. Lessa, J. (2016). Synthesis, Antitubercular And Anticancer Activities Of P-Nitrophenylethylenediamine-Derived Schiff Bases. *Medicinal Chemistry*, 13(4), 391–397. <https://doi.org/10.2174/1573406412666161104123149>
77. Saadaoui, I., Krichen, F., Ben Salah, B., Ben Mansour, R., Miled, N., Bougatef, A., & Kossentini, M. (2019). Design, Synthesis And Biological Evaluation Of Schiff Bases Of 4-Amino-1,2,4-Triazole Derivatives As Potent Angiotensin Converting Enzyme Inhibitors And Antioxidant Activities. *Journal Of Molecular Structure*, 1180, 344–354. <https://doi.org/10.1016/J.Molstruc.2018.12.008>
78. Sadia, M., Khan, J., Naz, R., Zahoor, M., Wadood Ali Shah, S., Ullah, R., Naz, S., Bari, A., Majid Mahmood, H., Saeed Ali, S., Ansari, S. A., & Sohaib, M. (2021). Schiff Base Ligand L Synthesis And Its Evaluation As Anticancer And Antidepressant Agent. *Journal Of King Saud University - Science*, 33(2). <https://doi.org/10.1016/J.Jksus.2020.101331>
79. Saha, I., & Kumar, G. S. (2011). Spectroscopic Characterization Of The Interaction Of Phenosafranin And Safranin O With Double Stranded, Heat Denatured And Single Stranded Calf Thymus DNA. *Journal Of Fluorescence*, 21(1), 247–255. <https://doi.org/10.1007/S10895-010-0712-3>
80. Saitou, N. (2018). Replication, Transcription, And Translation (Pp. 3–21). https://doi.org/10.1007/978-3-319-92642-1_1
81. Sánchez-González, Á., & Gil, A. (2021). Elucidating The Intercalation Of Methylated 1,10-Phenanthroline With DNA: The Important Weight Of The Ch/H Interactions And The Selectivity Of Ch/II And Ch/N Interactions. *Rsc Advances*, 11(3), 1553–1563. <https://doi.org/10.1039/D0ra07646e>
82. Shahabadi, N., Kashanian, S., Khosravi, M., & Mahdavi, M. (2010). Multispectroscopic Dna Interaction Studies Of A Water-Soluble Nickel(II) Complex Containing Different Dinitrogen Aromatic Ligands. *Transition Metal Chemistry*, 35(6), 699–705. <https://doi.org/10.1007/S11243-010-9382-X>
83. Sharma, M., Chauhan, K., Srivastava, R. K., Singh, S. V., Srivastava, K., Saxena, J. K., Puri, S. K., & Chauhan, P. M. S. (2014). Design And Synthesis Of A New Class Of 4-Aminoquinolonyl- And 9-Anilinoacridonyl Schiff Base Hydrazones As Potent Antimalarial Agents. *Chemical Biology And Drug Design*, 84(2), 175–181. <https://doi.org/10.1111/Cbdd.12289>
84. Silvestri, C., & Brodbelt, J. S. (2013). Tandem Mass Spectrometry For Characterization Of Covalent Adducts Of DNA With Anticancer Therapeutics. In *Mass Spectrometry Reviews* (Vol. 32, Issue 4, Pp. 247–266). <https://doi.org/10.1002/Mas.21363>
85. Sirajuddin, M., Ali, S., & Badshah, A. (2013). Drug-DNA Interactions And Their Study By UV-Visible, Fluorescence Spectroscopies And Cyclic Voltametry. In *Journal Of Photochemistry And Photobiology B: Biology* (Vol. 124, Pp. 1–19). <https://doi.org/10.1016/J.Jphotobiol.2013.03.013>
86. Sirajuddin, M., Ali, S., Haider, A., Shah, N. A., Shah, A., & Khan, M. R. (2012). Synthesis, Characterization, Biological Screenings And Interaction With Calf Thymus DNA As Well As Electrochemical Studies Of Adducts Formed By Azomethine [2-((3,5-Dimethylphenylimino)Methyl)Phenol] And Organotin(IV) Chlorides. *Polyhedron*, 40(1), 19–31. <https://doi.org/10.1016/J.Poly.2012.03.048>
87. Sirajuddin, M., Ali, S., Shah, N. A., Khan, M. R., & Tahir, M. N. (2012). Synthesis, Characterization, Biological Screenings And Interaction With Calf Thymus DNA Of A Novel Azomethine 3-((3,5-Dimethylphenylimino)Methyl)Benzene-1,2-Diol. *Spectrochimica Acta - Part A: Molecular And Biomolecular Spectroscopy*, 94, 134–142. <https://doi.org/10.1016/J.Saa.2012.03.068>
88. Szatyłowicz, H., Jezuita, A., Ejsmont, K., & Krygowski, T. M. (2017). Classical And Reverse Substituent Effects In Meta- And Para-Substituted Nitrobenzene Derivatives. *Structural Chemistry*, 28(4), 1125–1132. <https://doi.org/10.1007/S11224-017-0922-2>
89. Takenaka, S. (2017). Modified Naphthalene Diimide As A Suitable Tetraplex DNA Ligand: Application To Cancer Diagnosis And Anti-Cancer Drug. *International Conference On Nano-Bio Sensing, Imaging, And Spectroscopy 2017*, 10324, 103240g. <https://doi.org/10.1117/12.2271575>
90. Tanaka, M., Elias, B., & Barton, J. K. (2010). DNA-Mediated Electron Transfer In Naphthalene-Modified Oligonucleotides. *Journal Of Organic Chemistry*, 75(8), 2423–2428. <https://doi.org/10.1021/Jo1000862>
91. Thomas, A. B., Tupe, P. N., Badhe, R. V., Nanda, R. K., Kothapalli, L. P., Paradkar, O. D., Sharma, P. A., & Deshpande, A. D. (2009). Green Route Synthesis Of Schiff's Bases Of Isonicotinic Acid Hydrazide. *Green Chemistry Letters And Reviews*, 2(1), 23–27. <https://doi.org/10.1080/17518250902922798>
92. Tidwell, T. T. (2008). Hugo (Ugo) Schiff, Schiff Bases, And A Century Of β -Lactam Synthesis. In *Angewandte Chemie - International Edition* (Vol. 47, Issue 6, Pp. 1016–1020). <https://doi.org/10.1002/Anie.200702965>
93. Torres, P. H. M., Sodero, A. C. R., Jofily, P., & Silva-Jr, F. P. (2019). Key Topics In Molecular Docking For Drug Design. In *International Journal Of Molecular Sciences* (Vol. 20, Issue 18). [Mdpi Ag. https://doi.org/10.3390/Ijms20184574](https://doi.org/10.3390/Ijms20184574)

94. Travers, A., & Muskhelishvili, G. (2015). DNA Structure And Function. In Febs Journal (Vol. 282, Issue 12, Pp. 2279–2295). Blackwell Publishing Ltd. <https://doi.org/10.1111/febs.13307>
95. Udenfriend, S., & Zaltzman, P. (1962). Fluorescence Characteristics Of Purines, Pyrimidines, And Their Derivatives: Measurement Of Guanine In Nucleic Acid Hydrolyzates.
96. Wei, H., Lv, M., Duan, X., Li, S., Yao, Y., Wang, K., Zhang, P., Li, X., & Chen, H. (2014). Cytotoxicity And DNA-Binding Property Of Water-Soluble Naphthalene Diimide Derivatives Bearing 2-Oligoethoxy Ethanamine Side Chain End-Labeled With Tertiary Amino Groups. Medicinal Chemistry Research, 23(5), 2277–2286. <https://doi.org/10.1007/S00044-013-0823-X>
97. Yanthan, S., & Bhattacharyya, J. (2023). On Binding Mechanism Exploration Of Organic Amphoteric Dye Rhodamine B With Natural Polymeric DNA. Discover Materials, 3(1). <https://doi.org/10.1007/S43939-023-00043-9>
98. Yaseen, A. A., Al-Tikrity, E. T. B., El-Hiti, G. A., Ahmed, D. S., Baashen, M. A., Al-Mashhadani, M. H., & Yousif, E. (2021). A Process For Carbon Dioxide Capture Using Schiff Bases Containing A Trimethoprim Unit. Processes, 9(4). <https://doi.org/10.3390/pr9040707>
99. Yurtaş, L., Özkay, Y., Kaplancikli, Z. A., Tunali, Y., & Karaca, H. (2013). Synthesis And Antimicrobial Activity Of Some New Hydrazone-Bridged Thiazole-Pyrrole Derivatives. Journal Of Enzyme Inhibition And Medicinal Chemistry, 28(4), 830–835. <https://doi.org/10.3109/14756366.2012.688043>
100. Zeraati, M., Langley, D. B., Schofield, P., Moye, A. L., Rouet, R., Hughes, W. E., Bryan, T. M., Dinger, M. E., & Christ, D. (2018). I-Motif DNA Structures Are Formed In The Nuclei Of Human Cells. Nature Chemistry, 10(6), 631–<https://doi.org/10.1038/S41557-018-0046-3>
101. Zhang, C., Zhao, J., Lu, B., Seeman, N. C., Sha, R., Noinaj, N., & Mao, C. (2023). Engineering DNA Crystals a-Guest Molecule Interactions. Journal Of The American Chemical Society, 145(8), 4853–4859. <https://doi.org/10.1021/jacs.3c00081>
102. Zhitnikova, M. Yu., & Shestopalova, A. V. (2017). Protein-DNA Complexation: Contact Profiles In Dna Grooves. Biophysical Bulletin. <https://doi.org/10.26565/2075-3810-2017-38-06>

Declaration of Competing Interest

All authors have made significant contributions to the manuscript. Specifically: **Sofian S. Mohamed**: Conceived and designed the study, performed chemical synthesis, interpreted data, and wrote the original draft. **Salah M. Bensaber** provided supervision, contributed to the study's conception and design, and assisted with interpreting chemical spectra. **Nisreen H. Meiqal, Hamza S. Atiya, Mohamed A. Ahmed and Anton Hermann**: Contributed through reviewing and editing the manuscript. **Abdul M. Gbaj**: Supervised the biological screening, reviewed and validated data, and contributed to drafting the manuscript.

All authors have reviewed and approved the final version of the manuscript. Furthermore, this manuscript has not been submitted to, nor is it under consideration by, any other journal or publishing venue.

Acknowledgments

We would like to thank the team of Judicial Expertise and Research Center, Tripoli, Libya for technical support throughout this project. We also thank Sir consultant Khaled Abuajila Diab (CEO of Judicial Expertise and Research Center, Tripoli, Libya) for his valuable support while performing this project.

Ethical approval

All the methods were performed under relevant institutional guidelines and regulations.

Appendix A. Supplementary material

Supplementary data associated with the article can be found in the online version.

Supplementary material

Table 4A: Modeling Data of the Reported Compounds on DNA Fragment 1K2J.

Codes	ΔG	DNA Residues Involved in Interaction	Number & type of bonds Involved in Interaction
INH01	-7.1	O4-Gua12, O2-Thy13	(2) C-H bonds.
INH02	-7.5	N3-Ade4, O2-Thy3, H22-Gua2, N3-Ade4, H1-Thy3	(3) Conventional H bond, (2) C-H bond.
INH03	-8.4	N3-Ade4, H22-Gua8, H1-Gua6, H4-Cyt11, O2-Cyt11, O2-Thy3	(2) Conventional H bond, (4) C-H bond.
INH04	-7.4	N3-Ade4, H2-Ade4, Op1-Cyt11	(1) Conventional H bond, (2) C-H bond.
INH05	-7.6	Phenylring-Cyt5, N3-Ade10, N3-Ade4, H21-Gua8, H22-Gua8, Op1-Cyt5, H2-Ade10, H4-Ade6	(4) Conventional H bond, (3) C-H bonds. (1) pi-pi stacked hydrophobic.
INH06	-7.2	N3-Gua12, O2-Cyt11, H4-Cyt5, H22-Gua2, O2-Thy3, Phenylring-Gua2, Phenylring-Cyt5, Phenylring-Ade4, Phenylring-Ade10, 5ring-Ade10	(1) Conventional H bond, (3) C-H bonds. (1) pi-pi T-shaped hydrophobic. (1) pi-donor H bond. (4) pi-alkyl hydrophobic.
INH07	-7.6	N3-Ade4, N3-Ade10, H2-Ade4, O4-Ade4, O3-Thy3, O4-Gua12, Op1-Cyt11	(2) Conventional H bond. (4) C-H bonds.

			(1) pi-anion electrostatic bond.
INH08	-7.7	H21-Gua2, N3-Ade4, H2-Ade4	(2) Conventional H bond, (1) C-H bond.
INH09	-8.6	O2-Cyt11, O4-Cyt5, Phenylring-Cyt11, O2-Thy3, H2-Ade4	(2) Conventional H bond, (2) C-H bond. (1) pi-pi stacked hydrophobic. (1) pi-pi T-shaped hydrophobic.
INH10	-8.2	N3-Ade10, H22-Gua8, H2-Ade10, H4-Ade10	(2) Conventional H bond, (2) C-H bond.
INH11	-8.2	5ring-Ade10, O2-Thy9, O2-Cyt5, H4-Cyt5, N3-Ade4, H22-Gua2, O3-Ade4	(3) Conventional H bond, (4) C-H bond. (1) pi-pi T-shaped hydrophobic.
INH12	-8.2	N3-Ade10, H22-Gua8, H2-Ade10, H4-Ade10	(2) Conventional H bond, (2) C-H bond.
INH13	-7.1	O2-Thy3, H2-Ade4, Op1-Cty11	(1) Conventional H bond, (3) C-H bond.
INH14	-8.9	N3-Ade4, H2-Ade4, O4-Gua12, O3-Thy3	(1) Conventional H bond, (3) C-H bond.
INH15	-7.4	O2-Thy9, N3-ade10, H5-Gua6	(1) Conventional H bond, (2) C-H bond.
INH16	-6.9	N3-Ade10, O2-Thy9, O2-Cyt5, Phenylring-Cyt11	(1) Conventional H bond, (2) C-H bond. (1) Pi-Sulfur bond.
INH17	-7.2	O2-Thy3, Phenylring-Cyt11, Phenylring-Cyt5, H5-Gua12, N3-Ade4	(1) Conventional H bond, (2) C-H bond. (1) pi-pi stacked hydrophobic
INH18	-6.8	N3-Ade10, OP1-Cyt5	(1) Conventional H bond, (1) C-H bonds. (1) pi-anion electrostatic bond.
INH19	-8.6	O2-Thym3, O2-Cyt11, N3-Ade10	(1) Conventional H bond, (3) C-H bond.
INH	-5.4	H2-Ade4, H2-Ade10	(2) C-H bond. (1) pi-pi T-shaped hydrophobic.
PT	-6.3	Op2-Gua8, Op2-Thy3, H24-Cyt7, H6-Thy3, Phenylring-Cyt5.	(3) Conventional H bond, (1) C-H bonds. (1) pi-pi T-shaped hydrophobic.

Abbreviations: The table includes several key abbreviations to represent various atoms and molecular components relevant to DNA structure. "O" stands for an oxygen atom, "H" denotes a hydrogen atom, "N" refers to a nitrogen atom, "Op" specifically represents an oxygen atom within a phosphate group, and "C" is used for a carbon atom. The nucleobases are also abbreviated, with "Cyt" representing cytosine, "Ade" for adenine, "Thy" for thymine, and "Gua" for guanine, all of which are essential components of DNA.

Table 4B: Modeling Data of the Reported Compounds on DNA Fragment 1ZEW.

Codes	ΔG	DNA Residues Involved in Interaction	Number & type of bonds Involved in Interaction
INH01	-7.2	Op1-Gua17, O4-Ade6, O2-Thy5, O4-Thy5, O3-Ade18, Phenylring-Ade18	(3) Conventional H bond, (2) C-H bonds. (1) pi-pi T-shaped hydrophobic.
INH02	-7.5	N3-Ade8, O4-Ade8, O4-Ade16, O2-Thy15	(4) Conventional H bond. (1) unfavorable acceptor-acceptor.
INH03	-8.7	N2-Gua7, N3-Ade16, N2-Gua17, Phenylring-Ade8, Phenylring-Gua17	(3) Conventional H bond, (2) C-H bond. (2) pi-pi T-shaped hydrophobic.
INH04	-7.4	O2-Thy5, O4-Ade6, Phenylring-Ade18, N2-Gua17, Phenylring-Gua19	(2) Conventional H bond, (1) unfavorable donor-donor, (2) pi-alkyl hydrophobic. (1) pi-pi T-shaped hydrophobic.
INH05	-7.8	O2-Thy5, O2ade6, O4-Gua19, O4-Thy5, N2-Gua17	(3) Conventional H bond, (1) C-H bonds. (1) unfavorable donor-donor.
INH06	-7.9	O2-Thy5, O4-Ade6, O4-Gua19, O4-Thy5, N2-Gua17, Phenylring-Gua19	(3) Conventional H bond, (1) C-H bonds. (1) unfavorable donor-donor, (1) pi-alkyl hydrophobic.
INH07	-8.0	O4-Ade6, C1-Ade16, O2-Gua7, N2-Gua7, O2-Cyt14, Phenylring-Gua7, 5ring-Ade6	(1) Conventional H bond, (4) C-H bonds, (1) pi-pi T-shaped hydrophobic.

			(2) pi-pi stacked hydrophobic.
INH08	-7.5	O2-Thy5, O4-Ade6, O4-Thy5, Phenylring-Gua19, 5ring-Gua19, N2-Gua17	(2) Conventional H bond, (1) C-H bond. (2) pi-alkyl hydrophobic, (2) unfavorable donor-donor.
INH09	-8.4	O4-Ade6, N2-Gua17, O2-Thy5, C2-Ade16, O4-Thy5, Phenylring-Ad18	(4) Conventional H bond, (2) C-H bond. (1) pi-pi T-shaped hydrophobic.
INH10	-8.3	N2-Gua7, N3-Ade8, N2-Gua9, N3-Ade16, Phenylring-Gua9	(3) Conventional H bond, (1) C-H bond. (1) pi-pi T-shaped hydrophobic.
INH11	-8.5	C2-Ade6, N2-Gua7, O4-Ade6, N3-Ade16, O3-Ade16, O4-Gua17, Phenylring-Ade6, Phenylring-Gua17, Phenylring-ADE16, Phenylring-ADE8	(5) Conventional H bond, (1) C-H bond. (3) pi-pi T-shaped hydrophobic. (1) pi-alkyl hydrophobic.
INH12	-8.4	N3-Ade16, O2-Cyt17, Phenylring-Gua9, N2-Gua7, O2-Cyt14, N2-Gua9	(3) Conventional H bond, (1) C-H bond. (1) pi-pi T-shaped hydrophobic. (1) unfavorable donor-donor.
INH13	-6.9	O2-Thy5, O4-Ade6, N2-Gua17, N2-Gua17	(3) Conventional H bond, (1) unfavorable donor-donor.
INH14	-8.9	N2-GUA7, O2-ADE16	(2) Conventional H bond, (1) C-H bond.
INH15	-7.2	N3-Ade6, O4-Ade6, OP1-Gua17, C5-Ade18, 5ring-Ade8, Phenylring-Ade8	(3) Conventional H bond, (1) C-H bond. (2) pi-alkyl hydrophobic
INH16	-6.4	N2-Gua17, O2-Thy5, O4-Ade6, O4-Thy5, N2-Gua17	(3) Conventional H bond, (1) C-H bond. (1) unfavorable donor-donor
INH17	-7.6	O2-Thy5, O5-Gua19, N3-Ade18, N2-Gua17, N2-Gua19, 5ring-Gua19, Phenylring-Gua19, Phenylring-Gua18	(4) Conventional H bond, (1) pi-donor H bond, (1) pi-pi T-shaped hydrophobic.
INH18	-7.7	OP1-Gua17, O3-Ade16, O4-Ade6, O2-Thy5, O4-Gua17, Phenylring-Ade16	(4) Conventional H bond, (1) C-H bonds. (1) pi-pi T-shaped hydrophobic.
INH19	-8.9	N2-Gua7, O4-Thy15, O2-Cyt14	(3) Conventional H bond.
INH	-5.9	O4-Gua20, N2-Gua17, O4-Thy5, O2-Cyt4, Phenylring-Ade18, Phenylring-Gua19, 5ring-Gua19	(4) Conventional H bond, (1) C-H bond. (3) pi-pi T-shaped hydrophobic.
PT	-8.6	N2-Gua17, N2-Gua19, Phenylring-Ade6	(2) Conventional H bond. (1) pi-pi T-shaped hydrophobic.

Abbreviations: The table includes several key abbreviations to represent various atoms and molecular components relevant to DNA structure. "O" stands for an oxygen atom, "H" denotes a hydrogen atom, "N" refers to a nitrogen atom, "Op" specifically represents an oxygen atom within a phosphate group, and "C" is used for a carbon atom. The nucleobases are also abbreviated, with "Cyt" representing cytosine, "Ade" for adenine, "Thy" for thymine, and "Gua" for guanine, all of which are essential components of DNA.

Table 4C: Modeling Data of the Reported Compounds on DNA Fragment 102D.

Codes	ΔG	DNA Residues Involved in Interaction	Number & type of bonds Involved in Interaction
INH01	-7.00	O4-Gua18, O2-Thy9	(3) Conventional H bond, (1) pi-donor H bonds. (1) pi-pi T-shaped hydrophobic
INH02	-7.3	O2-Thy7, C2-Ade6, O2-Thy8	(1) Conventional H bond (1) pi-anion electrostatic, (2) C-H bonds.
INH03	-8.5	N3-Ade18, O2-Thy9	(1) Conventional H bond, (1) C-H bonds.
INH04	-7.6	C2-Ade17, O2-Thy9	(1) Conventional H bond, (1) C-H bonds.
INH05	-7.8	N3-Ade17, O2-Thy9, O3-Ade17, C4-Thy8, O2-Thy19, Phenylring-Thy18	(2) Conventional H bond. (4) C-H bonds, (1) pi-alkyl hydrophobic
INH06	-7.9	O3-Ade17, N3-Ade18, N3-Ade17, O2-Thy9	(2) Conventional H bond, (2) C-H bonds.
INH07	-7.8	O2-Thy8, C2-Ade17, O4-Thy8	(1) Conventional H bond, (2) C-H bonds.
INH08	-7.8	C2-Ade17, O3-Ade17, O2-Thy9, O4-Gua10	(2) Conventional H bond, (2) C-H bonds.
INH09	-8.4	O2-Thy9, O3-Ade18, C3-Ade18, C3-Thy8	(2) Conventional H bond, (2) C-H bonds.

			(1) pi-anion electrostatic.
INH10	-8.3	O4-Thy7, O4-Thy20, O4-Ade6, C5-Thy21, O2-Thy7, C4-Thy20	(2) Conventional H bond, (4) C-H bonds.
INH11	-8.4	O4-Thy9, Phenylring-Ade18, O2-Ade17, O4-Ade18, N3-Ade18, O2-Thy19	(1) Conventional H bond, (4) C-H bonds. (1) pi-alkyl hydrophobic.
INH12	-8.3	O2-Thy8, C2-Ade17	(1) Conventional H bond, (1) C-H bonds.
INH13	-7.0	O2-Thy9, N3-Ade18, O3-Ade17	(1) Conventional H bond, (2) C-H bonds.
INH14	-9.1	O4-Ade18, O4-Gua10, O3-Cyt11	(1) Conventional H bond, (3) C-H bonds.
INH15	-7.3	O2-Thy9, N3-Ade18, O2-Thy8	(1) Conventional H bond, (2) C-H bonds.
INH16	-6.9	O2-Thy8, C2-Ade17	(1) Conventional H bond, (1) C-H bonds.
INH17	-8.1	O2-Thy20, O2-Thy21, C2-Ade4, OP1-Thy7, O4-Ade6, N3-Ade6, OP1-Thy7	(2) Conventional H bond, (3) C-H bonds. (1) pi-anion electrostatic bond. (1) unfavorable acceptor – acceptor.
INH18	-7.2	O2-Thy9, O4-Thy9, N3-Ade18, O4-Ade18, O3-Ade17	(2) Conventional H bond, (3) C-H bonds.
INH19	-9.0	O2-Thy9, O4-Thy9, OP1-Thy20, OP1-Thy9, O3-Ade17, N3-Ade18	(2) Conventional H bond, (2) C-H bonds. (2) pi-anion electrostatic bond.
INH	-5.8	O4-Thy19, O2-Thy17, O4-Thy7, O2-Thy20, O4-Thy20	(5) Conventional H bond, (2) C-H bonds.
PT	-8.4	Op2-Ade17, O4-Thy19, N6-Ade5, N7-Ade4, C8-Ade4, Op2-Ade4, Op2-Cyt3, 5ring-Ade17, N6-Ade5, N4-Cyt3.	(4) Conventional H bond, (1) C-H bonds. (1) pi- sigma hydrophobic. (2) pi-anion electrostatic bond. (1) unfavorable donor-donor. (1) Pi-donor H bond.

Abbreviations: The table includes several key abbreviations to represent various atoms and molecular components relevant to DNA structure. "O" stands for an oxygen atom, "H" denotes a hydrogen atom, "N" refers to a nitrogen atom, "Op" specifically represents an oxygen atom within a phosphate group, and "C" is used for a carbon atom. The nucleobases are also abbreviated, with "Cyt" representing cytosine, "Ade" for adenine, "Thy" for thymine, and "Gua" for guanine, all of which are essential components of DNA.

Table 4D: Modeling Data of the Reported Compounds on DNA Fragment 3EYO.

Codes	ΔG	DNA Residues Involved in Interaction	Number & type of bonds Involved in Interaction
INH01	-6.7	O4-Thy4, O2-Thy4, O2-Thy8, O3-Ade3	(3) Conventional H bond, (1) C-H bonds.
INH02	-7.9	Op1-Ade7, O4-Ade7, O2-Thy6, N3-Ade7	(2) Conventional H bond, (1) C-H bonds. (1) pench bond electrostatic.
INH03	-8.6	C4-Thy8, O2-Thy6, C5-Thy8, O4-Ade5	(5) C-H bonds.
INH04	-7.4	O2-Thy6	(2) C-H bonds.
INH05	-7.8	O2-Thy6, N3-Ade5, O4-Ade5, C4-Thy8, Phenylring-Ade5, 5ring-Ade5, Phenylring-Ade7	(4) C-H bonds. (3) pi-alkyl hydrophobic.
INH06	-6.9	Op1-Ade9, O3-Thy8, Opi-Ade7, O2-Thy6, C2-Ade5, Op1-Thy8, Phenylring-Ade5, 5ring-Ade5, Phenylring-Ade7, Phenylring-Thy8	(4) Conventional H bond, (2) C-H bonds. (4) pi-alkyl hydrophobic.
INH07	-7.8	O2-Thy6, C2-Ade5, O4-Ade5, O3-Ade5	(1) Conventional H bond, (3) C-H bonds.
INH08	-7.0	Op1-Thy8, O3-Ade7, N3-Ade5, Phenylring-Thy4	(1) pi-stacked hydrophobic, (4) C-H bonds.
INH09	-7.7	O2-Thy8, O2-Thy4, N3-Ade5	(2) Conventional H bond. (1) unfavorable acceptor-acceptor.

INH10	-8.3	O2-Thy6(A), O2-Thy6(B), O4-Thy6(B), C4-Ade5, O4-Ade7	(3) Conventional H bond, (2) C-H bonds.
INH11	-8.8	O4-Thy6, N3-Ade5, O4-Ade7, C5-Thy8, O4-Ade5, Phenylring-Ade7, Phenylring-Ade5	(3) Conventional H bond, (2) C-H bonds. (2) pi-alkyl hydrophobic.
INH12	-8.4	O4-Ade7(A), O2-Thy6, O4-Ade7(B)	(2) Conventional H bond, (1) C-H bonds.
INH13	-6.5	N3-Ade5, Phenylring-Thy4	(2) C-H bonds. (2) pi- pi stacked hydrophobic.
INH14	-9.2	O4-Ade7, O2-Thy6, O4-Ade5, Op1-Thy8	(2) Conventional H bond, (1) C-H bonds. (1) pi- anion electrostatic.
INH15	-6.9	O2-Thym8, O2-Thy4, C4-Thy8, C4-Ade9, O2-Thy4	(2) Conventional H bond, (1) C-H bonds. (1) pi-sigma hydrophobic
INH16	-6.8	O2-Thy6, O2-Thy6	(2) C-H bonds.
INH17	-7.7	O2-Thy8, O2-Thy4, O2-Thy4, O4-Ade5, OP1-Thy6	(2) Conventional H bond, (2) C-H bonds. (1) pi-anion electrostatic bond.
INH18	-6.9	O2-Thy4, O2-Thy8, O4-Ade5, N3-Ade9, O3-Ade9, O2-Thy8	(3) Conventional H bond, (3) C-H bonds.
INH19	-8.8	O4-Ade7, O4-Ade7, O2-Thy6	(1) Conventional H bond, (2) C-H bonds.
INH	-5.6	O2-Thy4, O2-Thy4, O4-Ade5, O2-Thy8	(4) Conventional H bond.
PT	-6.3	O4-Thy6, N6-Ade5, Op2-Thy4, N7-Ade5.	(3) Conventional H bond. (1) pi- anion electrostatic. (1) unfavorable acceptor – acceptor.

Abbreviations: The table includes several key abbreviations to represent various atoms and molecular components relevant to DNA structure. "O" stands for an oxygen atom, "H" denotes a hydrogen atom, "N" refers to a nitrogen atom, "Op" specifically represents an oxygen atom within a phosphate group, and "C" is used for a carbon atom. The nucleobases are also abbreviated, with "Cyt" representing cytosine, "Ade" for adenine, "Thy" for thymine, and "Gua" for guanine, all of which are essential components of DNA.

Table 4E: Modeling Data of the Reported Compounds on DNA Fragment 330D.

Codes	ΔG	DNA Residues Involved in Interaction	Number & type of bonds Involved in Interaction
INH01	-6.5	N2-Gua23, O4-Gua4, O2-Cyt3	(3) Conventional H bond.
INH02	-6.8	O3-Cyt3, N2-Gua23, O4-Gua4, O2-Cyt3, N7-Gua22	(4) Conventional H bond, (1) C-H bonds.
INH03	-7.7	O4-Gua22, N2-Gua7, N2-Gua19, Phenylring-Gua7, N2-Gua19	(2) Conventional H bond, (1) C-H bonds. (1) pi-pi T-shaped hydrophobic. (1) unfavorable donor-donor.
INH04	-6.5	N2-Gua7, O2-Cyt18, N2-Gua8, N3-Gua8, Phenyl Ring-Gua10, 5 Ring-Gua10	(2) Conventional H bond. (1) pi-donor H bond. (1) unfavorable acceptor-acceptor. (2) pi-alkyl hydrophobic.
INH05	-7.1	O4-Gua19, N2-Gua20, N3-Gua20, O3-Gua20, N2-Gua7, O4-Gua8, N2-Gua7	(6) Conventional H bond, (1) C-H bonds. (1) pi-alkyl hydrophobic.
INH06	-7.1	N2-Gua8, N2-Gua16, O3-Cyt9, O5-Gua10	(3) Conventional H bond, (1) C-H bonds. (1) pi-pi stacked.
INH07	-7.5	O3-Cyt9, N2-Gua7, O4-Gua20, N3-Gua19, O4-Cyt9, N3-Gua8, N2-Gua19, O2-Cyt5, O4-Cyt6, O3-Cyt6	(4) Conventional H bond, (5) C-H bonds. (1) pi-alkyl hydrophobic.
INH08	-7.0	N2-Gua7, O2-Cyt18, O4-Cyt18, N2-Gua16, N2-Gua8, C1-Gua10, Phenylring-Gua10	(4) Conventional H bond, (2) C-H bonds. (1) pi-alkyl hydrophobic.
INH09	-7.9	O2-Gua23, N3-Gua4, O4-Cyt5, Phenylring-Gua23	(3) Conventional H bond, (1) C-H bonds.

			(1) pi-pi T-shaped hydrophobic.
INH10	-7.9	O4-Qua22, N2-Gua7, O3-Cyt21, N2-Gua19, Phenylring-Gua7,	(2) Conventional H bond, (1) C-H bonds. (1) pi-donor H bond. (1) pi-pi T-shaped hydrophobic. (1) unfavorable donor-donor.
INH11	-7.5	N2-Gua19, N2-Gua7, O4-Gua19, C4-Cyt9, N2-Gua8	(4) Conventional H bond, (1) C-H bonds. (1) pi-donor H bond
INH12	-8.0	N2-Gua7, O4-Gua19, O4-Cyt18, N2-Gua16, O2-Cyt18, O3-Gua19, N2-Gua8	(5) Conventional H bond, (1) C-H bonds. (1) pi-donor H bond.
INH13	-6.5	N2-Gua8, N2-Gua7, O2-Cyt18, O4-Gua19, O4-Gua20, N3-Gua7, N2-Gua19, O3-Gua8	(5) Conventional H bond, (4) C-H bonds.
INH14	-7.9	O3-Gua10, N2-Gua7, N2-Gua8, O2-Cyt18, O4-Cyt18	(4) Conventional H bond, (1) C-H bonds.
INH15	-7.2	O3-Gua8, O2-Cyt18, O4-Gua19, O4-Cyt18, N2-Gua8	(3) Conventional H bond, (1) C-H bonds. (1) pi-donor H bond.
INH16	-6.0	N3-Gua23, O4-Gua23, N2-Gua23, Phenylring-Gua23, O4-Thy24	(3) Conventional H bond, (1) C-H bonds. (1) pi-sulfur hydrophobic.
INH17	-7.2	N3-Gua4, O4-Cyt5, O3-Gua23	(3) Conventional H bond
INH18	-6.8	O4-Cyt5, N2-Gua4, N2-Gua23, O4-Thy24, Phenylring-Gua23	(1) Conventional H bond, (1) C-H bonds. (1) pi-donor H bond, (2) pi-pi T-shaped hydrophobic.
INH19	-8.1	O4-Cyt18, O2-Cyt18, N2-Gua8, N2-Gua7, N2-Gua16, N2-Gua8	(4) Conventional H bond. (2) pi-donor H bond.
INH	-5.1	N2-Gua8, O4-Gua19, O2-Cyt18, O4-Cyt18, N2-Gua7	(4) Conventional H bond. (1) pi-donor H bond.
PT	-7.6	O2-Cyt18, N2-Gua7	(1) Conventional H bond. (1) pi-donor H bond.

Abbreviations: The table includes several key abbreviations to represent various atoms and molecular components relevant to DNA structure. "O" stands for an oxygen atom, "H" denotes a hydrogen atom, "N" refers to a nitrogen atom, "Op" specifically represents an oxygen atom within a phosphate group, and "C" is used for a carbon atom. The nucleobases are also abbreviated, with "Cyt" representing cytosine, "Ade" for adenine, "Thy" for thymine, and "Gua" for guanine, all of which are essential components of DNA.

Table 4F: Modeling Data of the Reported Compounds on DNA Fragment 1BNA.

Codes	ΔG	DNA Residues Involved in Interaction	Number & type of bonds Involved in Interaction
INH01	-6.6	N2-Gua1-, O2-Cyt11	(2) Conventional H bond.
INH02	-6.8	N2-Gua16, N2-Gua10, O3-Cyt11, O2-Cyt11	(4) Conventional H bond.
INH03	-8.0	O2-Thy19, O2-Thy7, C5-Ade4, N3-Ade6, O2-Thy20, N2-Gua4	(3) Conventional H bond. (3) C-H bonds.
INH04	-7.1	N2-Gua14, N2-Gua10, N2-Gua16	(2) Conventional H bond. (1) pi-donor H bond.
INH05	-6.7	N3-Ade6, O2-Thy20	(2) Conventional H bond.
INH06	-6.8	N2-Gua2, O2-Cyt23, O4-Gua24, N2-Gua4, N2-Gua4, O4-Cyt23, 5Ring-Gua22	(5) Conventional H bond, (1) C-H bonds. (1) pi-donor H bond.
INH07	-7.5	N2-Gua10, N2-Gua16, N2-Gua14, N3-Gua12	(2) Conventional H bond, (3) C-H bonds.
INH08	-6.7	O4-Cyt21, N2-Gua22, O4-Gua22	(2) Conventional H bond, (2) C-H bonds.
INH09	-7.7	Op1-Cyt23, N2-Gua4, O2-Cyt21, O2-Thy20, N3-Ade6, C4-Ade6	(3) Conventional H bond, (3) C-H bonds.
INH10	-7.2	O2-Thy20, O4-Cyt21, C4-Thy20, N2-Gua4	(2) Conventional H bond, (1) C-H bonds. (1) pi-donor H bond.

INH11	-7.4	O2-Thy20, N2-Gua4, O2-Thy19, N3-Ade6	(2) Conventional H bond, (2) C-H bonds.
INH12	-7.4	O2-Thy20, N3-Ade6	(2) Conventional H bond.
INH13	-6.8	O3-Adse17, N2-Gua16, N2-Gua10, O2-Cyt11,	(4) Conventional H bond.
INH14	-8.8	N2-Gua16, O4-Cyt11, Op1-Gua10, Po1-Gua12, O3-Cyt9	(2) Conventional H bond, (1) C-H bonds. (2) pi-anion electrostatic bond.
INH15	-6.6	N2-Gua14, O2-Cyt11, O2-Cyt15, O2-Cyt11, N3-Gua16, N2-Gua10	(4) Conventional H bond, (1) C-H bonds. (1) unfavorable donor-donor
INH16	-6.6	N2-Gua16, N2-Gua10, O4-Gua16, N2-Gua14	(2) Conventional H bond, (2) C-H bonds.
INH17	-7.6	N2-Gua14, O2-Cyt11, O2-Cyt15, N2-Gua10, Phenylring-Cyt11	(3) Conventional H bond. (1) unfavorable donor-donor. (1) pi-sigma hydrophobic.
INH18	-6.9	O2-Cyt21, C5-Gua22, O2-Thy20, N3-Ade6, Phenylring- Gua4, N2-Gua22	(1) Conventional H bond, (3) C-H bonds. (1) pi-donor H bond. (1) pi-pi T-shaped hydrophobic.
INH19	-8.9	N2-Gua16, O4-Cyt11, Op1-Gua10	(2) Conventional H bond. (1) pi-anion electrostatic bond.
INH	-5.5	N2-Ade 10, N2-Ade 4	(2) Conventional H bond, (1) C-H bonds.
PT	-8.8	O6-Gua4, N7-Gua4, O4-Thy19, N6-Ade6, Op2-Ade17, Op2-Ade5, Phenylring-Cyt3, N7-Ade17, N6-Ade5, O4-Thy20	(5) Conventional H bond, (1) C-H bonds. (1) pi-anion electrostatic bond. (1) unfavorable donor-donor. (1) Pi-Pi T-shaped hydrophobic. (1) unfavorable acceptor - acceptor. (1) pi-sigma hydrophobic

Abbreviations: The table includes several key abbreviations to represent various atoms and molecular components relevant to DNA structure. "O" stands for an oxygen atom, "H" denotes a hydrogen atom, "N" refers to a nitrogen atom, "Op" specifically represents an oxygen atom within a phosphate group, and "C" is used for a carbon atom. The nucleobases are also abbreviated, with "Cyt" representing cytosine, "Ade" for adenine, "Thy" for thymine, and "Gua" for guanine, all of which are essential components of DNA.

Table 4G: Modeling Data of the Reported Compounds on DNA Fragment 2DNA.

Codes	ΔG	DNA Residues Involved in Interaction	Number & type of bonds Involved in Interaction
INH01	-6.6	N2-Gua10, O2-Thym9, O4-Gua12	(1) Conventional H bond, (2) C-H bonds.
INH02	-6.8	N2-Gua10, O4-Ade17, O3-Ade17, O4-Ade17	(4) Conventional H bond.
INH03	-8.0	N3-Ade16, O4-Ade17, N3-Gua10, C5-Thy19	(2) Conventional H bond, (2) C-H bonds.
INH04	-7.1	N2-Gua10	(1) Conventional H bond.
INH05	-6.7	N2-Gua10, O3-Thy9, O4-Gua10, O4-Gua12, Phenylring-Ade18, O4-Ade18	(3) Conventional H bond, (2) C-H bonds, (1) Pi-alkyl bond.
INH06	-6.8	N2-Gua10, O3-Thy9, O2-Gua12, O3-Ade18, O4-Gua10, Phenyl Ring-Ade18, 5Ring-Ade18	(2) Conventional H bond, (2) C-H bonds. (2) Pi-alkyl bond, (1) Unfavorable acceptor-acceptor.
INH07	-7.5	C2-Ade16, O3-Cyt11, N3-Gua12, Phenyl Ring-Gua12, N2-Gua14	(3) C-H bonds, (2) Pi-alkyl bond, (1) Pi-donor H bond.
INH08	-6.7	N2-Gua14, O3-Cyt11, O4-Ade16	(1) Conventional H bond, (2) C-H bonds.
INH09	-7.7	N2-Gua10, O4-Cyt11, O3-Ade17, O4-Gua12, O2-Thy9, N3-Ade17	(3) Conventional H bond, (3) C-H bonds.
INH10	-7.2	O4-Ade18, O4-Thy9, N3-Ade18, Op1-Gua10,	(2) Conventional H bond, (2) C-H bonds.

		C4-Thy19	(1) Pi-sigmahydrophobicbond.
INH11	-7.4	O3-Thy9, O2-Thy9, O4-Ade17, O2-Cyt15, N3-Ade16, O4-Gua10, C5-Ade18, Op1-Ade17, Phenylring-Thy9	(5) Conventional H bond, (3) C-H bonds, (1) Pi-Pi T-shaped hydrophobic.
INH12	-7.4	O3-Ade18, O4-Ade17, C1-Gua10	(2) Conventional H bond, (1) C-H bonds
INH13	-6.8	N2-Gua10, O2-Thy9, N3-Gua10, C2-Ade16, N3-Ade18	(3) Conventional H bond, (2) C-H bonds
INH14	-8.8	O4-Ade18, O2-Thy9, O4-Thy9, Op2-Gua10, Op1-Thy19, C4-Thy19, O3-Ade17, C1-Thy9, O3-Ade18, N3-Ade18, Op1-Thy20, O3-Thy19, O3-Thy8	(3) Conventional H bond, (7) C-H bonds. (2) pi-anion electrostatic bond, (1) pi-sigma hydrophobic.
INH15	-6.6	O2-Cyt15, O3-Cyt11, O2-Cyt15, N3-Ade16, Phenylring-Ade17	(2) Conventional H bond, (2) C-H bonds. (1) Pi-alkyl bond.
INH16	-6.6	O2-Thy9, O4-Cyt11, Op1-Gua10	(2) Conventional H bond, (1) pi-anion electrostatic bond.
INH17	-7.6	N2-Gua14, O2-Cyt15, O2-Cyt11, C1-Cyt15, N3-Ade16	(3) Conventional H bond, (2) C-H bonds. (1) unfavorable donor-donor.
INH18	-6.9	O4-Ade16, O2-Cyt15	(1) Conventional H bond, (1) C-H bonds.
INH19	-8.9	O4-Ade18, O4-Thy9, O2-Thy8, C4-Thy19, C5-Thy20, O4-Ade17	(3) Conventional H bond, (1) C-H bonds (2) pi-sigma hydrophobic.
INH	-5.5	N2-Ade 10, N2-Ade 4	(3) Conventional H bond.
PT	-8.3	Op2-Ade17, O4-Thy19, O4-Thy20, C6-Cyt3, C8-Ade4, N4-Cyt3, Phenylring-Cyt3, Op1-Ade4, Op2-Cyt3, 5ring-Ade17, N6-Ade5, N6-Ade4	(3) Conventional H bond, (2) C-H bonds. (2) Pi-anion electrostatic bond, (1) Pi-donor H bond, (1) Pi-Pi T-shaped hydrophobic, (1) pi-sigma hydrophobic, (3) unfavorable donor-donor.

Abbreviations: The table includes several key abbreviations to represent various atoms and molecular components relevant to DNA structure. "O" stands for an oxygen atom, "H" denotes a hydrogen atom, "N" refers to a nitrogen atom, "Op" specifically represents an oxygen atom within a phosphate group, and "C" is used for a carbon atom. The nucleobases are also abbreviated, with "Cyt" representing cytosine, "Ade" for adenine, "Thy" for thymine, and "Gua" for guanine, all of which are essential components of DNA.

Table 4H: Modeling Data of the Reported Compounds on DNA Fragment 181D.

Codes	ΔG	DNA Residues Involved in Interaction	Number & type of bonds Involved in Interaction
INH01	-6.4	O2-Cyt9, Op2-Gua12, N2-Gua10	(2) Conventional H bond (1) pi-donor H bonds.
INH02	-7.1	O2-Cyt1, O2-Thy11, Op2-Gua12, O2-Cyt9, N2-Gua10	(4) Conventional H bond, (1) C-H bond.
INH03	-7.1	N2-Gua10, O3-Cyt3, O2-Cyt3, C5-Ade2, C1-Cyt1	(3) Conventional H bond, (3) C-H bond.
INH04	-6.9	Phenyl Ring-Cyt9, C5-Gua4, Op2-Gua4, Op2-Cty12, O3-Cyt9, Op2-Gua10, N2-Gua4, Op2-Gua4	(4) Conventional H bond, (1) C-H bond. (2) pi-anion electrostatic bond. (1) pi-pi T-shaped hydrophobic.
INH05	-6.8	Op2-Gua4, C5-Gua4, N2-Gua4, Op2-Gua4, O2-Thy11, O3-Cyt9, Op2-Gua10	(5) Conventional H bond, (1) C-H bonds. (1) pi-anion electrostatic bond.
INH06	-7.1	O3-Cyt9, Op2-Gua10, N2-Gua4, Op2-Gua4, C5-Gua4, O3-Thy11, O2-Thy11, Phenyl Ring OfCyp	(4) Conventional H bond, (3) C-H bonds. (1) pi-pi T-shaped hydrophobic.
INH07	-7.2	Op2-Gua12, Op2-Gua4, O2-Cyt1, O2-Thy11, C5-Gua4, Phenylring-Cyt9, O3-Cyt9, Op2-Gua10, N2-Gua4, Op2-Gua4	(4) Conventional H bond, (3) C-H bonds. (1) pi-pi T-shaped hydrophobic. (2) pi-anion electrostatic bond.

INH08	-6.9	Op2-Gua12, Op2-Gua4, C5-Gua4, O2-Cyt1, N2-Gua4, Op2-Gua4, Op2-Gua10, O3-Cyt9,	(4) Conventional H bond, (3) C-H bond. (2) pi-anion electrostatic bond.
INH09	-7.4	Op1-Gua12, N2-Gua10, Phenyl Ring-Thy11, O2-Cyt1, O2-Cyt3, Op2-Gua4	(3) Conventional H bond. (1) pi-anion electrostatic bond. (1) unfavorable donor-donor. (1) pi-pi T-shaped hydrophobic.
INH10	-7.2	N2-Gua8, Op2-Gua10, O2-Cyt9, O3-Cyt9, Op2-Gua6, Op2-Gua8, Op2-Thy11	(4) Conventional H bond, (2) C-H bond. (2) pi-anion electrostatic bond.
INH11	-7.2	O2-Cyt3, O2-Thy11, O3-Cyt9, O2-Cyt3, O2-Cyt9, N2-Gua10, O3-Cyt1	(6) Conventional H bond, (1) C-H bond.
INH12	-7.1	N2-Gua10, O3-Cyt3, O2-Cyt3, N2-Gua12	(4) Conventional H bond.
INH13	-7.5	C5-Gua10, O3-Cyt5, O2-Cyt5, Op2-Gua4, Op2-Gua10, O3-Cyt9, N2-Gua8, N2-Gua10	(5) Conventional H bond, (3) C-H bond.
INH14	-7.4	Op2-Ade2, O2-Cyt3, O3-Cyt1, Op2-Thy11, Op1-Gua6	(2) Conventional H bond, (2) C-H bond. (1) pi-anion electrostatic bond.
INH15	-6.5	N2-Gua10, O3-Cyt9, OP2-Gua10, O2-Cyt9, OP2-Gua6, OP1-Gua6	(3) Conventional H bond, (1) C-H bond. (2) pi-anion electrostatic bond.
INH16	-6.9	OP1-Gua10, C5-Gua10, O2-Cyt5, O3-Cyt5, OP2-Gua4, N2-Gua10, OP2-Gua10, O3-Cyt9	(4) Conventional H bond, (3) C-H bond. (1) pi-anion electrostatic bond.
INH17	-6.8	O2-Cyt7, N2-Gua10, C5-Gua10, N2-Gua4	(2) Conventional H bond, (1) C-H bond. (1) pi-donor H bonds.
INH18	-6.8	OP2-Gua10, O3-Cyt9, Phenylring-Cyt9	(2) Conventional H bond. (1) pi-pi T-shaped hydrophobic.
INH19	-7.6	O2-Thy11, O2-Cyt3, O3-Cyt1, Op2-Ade2	(2) Conventional H bond, (2) C-H bond.
INH	-5.0	Phenyl Ring-Cyt9, C5-Gua4, Op2-Gua10, O3-Cyt9, N2-Gua4, Op1-Gua6, Op2-Gua4	(5) Conventional H bond, (2) C-H bond. (1) pi-pi T-shaped hydrophobic.
PT	-5.8	O2-Thy11, O2-Cyt1, N2-Gua12, O2-Cyt1, Op2-Gua12, N2-Gua12, C5-Gua12	(5) Conventional H bond, (1) C-H bond. (1) pi-anion electrostatic bond, (1) unfavorable donor-donor.

Abbreviations: The table includes several key abbreviations to represent various atoms and molecular components relevant to DNA structure. "O" stands for an oxygen atom, "H" denotes a hydrogen atom, "N" refers to a nitrogen atom, "Op" specifically represents an oxygen atom within a phosphate group, and "C" is used for a carbon atom. The nucleobases are also abbreviated, with "Cyt" representing cytosine, "Ade" for adenine, "Thy" for thymine, and "Gua" for guanine, all of which are essential components of DNA.

Table 4J: Modeling Data of the Reported Compounds on DNA Fragment 5MVK.

Codes	ΔG	DNA Residues Involved in Interaction	Number & type of bonds Involved in Interaction
INH01	-6.2	Po2-Gua5, O6-Gua5, O6-Gua7, N4-Cyt4	(3) Conventional H bonds, (1) pi-donor H bonds, (1) pi-pi T-shaped hydrophobic
INH02	-6.5	Op2-Gua5, N4-Cyt6, O6-Gua5, O6-Gua7, O6-Gua9, N4-Cyt8, 5ring-Gua5	(4) Conventional H bond, (1) pi-pi T-shaped hydrophobic, (2) unfavorable donor-donor
INH03	-6.8	O4-Thy2, O6-Gua9, N4-Cyt4, N4-Cyt8, N4-Cyt6, Phenylring-Thy10, C7-Thy10	(5) Conventional H bond, (1) pi-sigma hydrophobic, (1) pi-pi T-shaped hydrophobic
INH04	-6.1	Op2-Thy2, N4-Cyt4, N4-Cyt6, O6-Gua7,	(4) Conventional H bond.
INH05	-6.8	Op2-Thy2, N4-Cyt4, N4-Cyt6, O6-Gua7, O4-Thy10, O4-Thy2, N6-Ade3, N6-Ade11, N4-Cyt8, 5ring-Gua9	(6) Conventional H bond, (5) unfavorable donor-donor, (1) pi-alkyl hydrophobic.

INH06	-6.5	Op2-Cyt8, N4-Cyt6, N4-Cyt4, O4-Thy2, Phenylring-Gua7, 5ring-Gua7, Phenylring-Thy2, 5ring-Ade3, C7-Thy12	(4) Conventional H bond, (2) pi-pi T-shaped hydrophobic, (1) pi-stacked hydrophobic, (1) pi-sigma hydrophobic, (2) pi-alkyl hydrophobic.
INH07	-6.7	Op2-Thy2, N4-Cyt6, N4-Cyt6, O4-Thy2, N7-Gua9, O4-Thy10	(4) Conventional H bond, (3) C-H bonds. (2) pi-alkyl hydrophobic.
INH08	-6.3	N4-Cyt4, Op2-Thy2, N4-Cyt4, Phenylring-Cyt4, 5ring-Gua5	(4) Conventional H bond, (2) pi-alkyl hydrophobic.
INH09	-7.3	N4-Cyt4, O6-Gua7, N7-Gua7, N4-Cyt6	(3) Conventional H bond, (1) unfavorable donor-donor.
INH10	-6.9	O6-Gua9, N4-Cyt4, Phenylring-Thy2, 5ring-Ade3, C7-Thy10	(2) Conventional H bond, (1) pi-sigma hydrophobic, (2) pi-alkyl hydrophobic
INH11	-7.0	N4-Cyt4, N6-Ade3, O4-Thy2, N6-Ade3, Op2-Cyt8, Op2-Ade3, Phenylring-Cyt8, Phenylring-Gua9, 5ring-Gua9	(4) Conventional H bond, (1) C-H bonds. (1) pi-pi T-shaped hydrophobic, (1) pi-anion electrostatic bond, (1) pi-alkyl hydrophobic.
INH12	-6.7	C7-Thy10, Phenylring-Gua7	(1) pi-pi T-shaped hydrophobic, (1) pi-sigma hydrophobic.
INH13	-5.7	N4-Cyt4, N4-Cyt8, N4-Cyt6, N4-Cyt6, N4-Cyt4, N4-Cyt8, Phenylring-Cyt4	(6) Conventional H bond, (2) pi-donor H bonds, (1) pi-pi T-shaped hydrophobic.
INH14	-7.4	Phenylring-Cyt4, N4-Cyt4, Phrnylring-Thy10, C7-Thy10, Op2-Thy2,	(2) pi-pi T-shaped hydrophobic, (1) pi-sigma hydrophobic. (1) pi-anion electrostatic bond.
INH15	-6.4	OP2-Gua5, O6-Gua7, OP2-Cyt6, 5ring-Gua5	(2) Conventional H bond, (1) C-H bonds. (1) pi-pi T-shaped hydrophobic.
INH16	-6.4	O6-Gua7, Phrnylring-Gua9, O4-Thy2, N2-Gua9	(1) Conventional H bond, (2) C-H bonds. (1) pi-pi T-shaped hydrophobic.
INH17	-7.1	O6-Gua7, OP2-Gua5, N4-Cyt4, OP2-Cyt6, 5ring-Gua5	(3) Conventional H bond, (1) C-H bonds. (1) pi-pi T-shaped hydrophobic.
INH18	-6.3	N4-Cyt4, O6-Gua7, O6-Gua5, N4-Cyt4, 5ring-Gua5	(3) Conventional H bond, (1) pi-donor H bonds, (1) pi-pi T-shaped hydrophobic.
INH19	-7.2	N4-Cyt6, O6-Gua7, 5ring-Gua5, Phenylring-Gua5, Phenylring-Cyt8, 5ring-Gua9.	(2) Conventional H bond, (4) pi-pi T-shaped hydrophobic.
INH	-4.7	Op2-Cyt4, N4-Cyt6, O6-Gua7, O6-Gua5, O6-Gua7	4) Conventional H bond.
PT	-10.5	N4-Cyt8, N4-Cyt4, N4-Cyt4, N6-Ade3, N7-Gua5, N4-Cyt6, Op2-Gua5, Op2-Thy2, N7-Ade3, O6-Gua7, 5ring-Gua7, Phenylring-Cyt6, 5ring-Gua5, N4-Cyt8, Op2-Thy2, O6-Gua5.	(6) Conventional H bond, (2) C-H bonds. (2) pi-pi T-shaped hydrophobic, (2) pi-anion electrostatic bond, (2) pi-donor H bonds, (2) unfavorable acceptor-acceptor.

Abbreviations: The table includes several key abbreviations to represent various atoms and molecular components relevant to DNA structure. "O" stands for an oxygen atom, "H" denotes a hydrogen atom, "N" refers to a nitrogen atom, "Op" specifically represents an oxygen atom within a phosphate group, and "C" is used for a carbon atom. The nucleobases are also abbreviated, with "Cyt" representing cytosine, "Ade" for adenine, "Thy" for thymine, and "Gua" for guanine, all of which are essential components of DNA.

Table 4K: Modeling Data of the Reported Compounds on DNA Fragment 3EYO.

Codes	ΔG	DNA Residues Involved in Interaction	Number & type of bonds Involved in Interaction
INH01	-6.7	O4-Thy4, O2-Thy4, O2-Thy8, O3-Ade3	(3) Conventional H bond, (1) C-H bonds.
INH02	-7.9	Op1-Ade7, O4-Ade7, O2-Thy6, N3-Ade7	(2) Conventional H bond, (1) C-H bonds. (1) pench bond electrostatic.
INH03	-8.6	C4-Thy8, O2-Thy6, C5-Thy8, O4-Ade5	(5) C-H bonds.
INH04	-7.4	O2-Thy6	(2) C-H bonds.
INH05	-7.8	O2-Thy6, N3-Ade5, O4-Ade5, C4-Thy8, Phenylring-Ade5, 5ring-Ade5, Phenylring-Ade7	(4) C-H bonds. (3) pi-alkyl hydrophobic.

INH06	-6.9	Op1-Ade9, O3-Thy8, Opi-Ade7, O2-Thy6, C2-Ade5, Op1-Thy8, Phenylring-Ade5, 5ring-Ade5, Phenylring-Ade7, Phenylring-Thy8	(4) Conventional H bond, (2) C-H bonds. (4) pi-alkyl hydrophobic.
INH07	-7.8	O2-Thy6, C2-Ade5, O4-Ade5, O3-Ade5	(1) Conventional H bond, (3) C-H bonds.
INH08	-7.0	Op1-Thy8, O3-Ade7, N3-Ade5, Phenylring-Thy4	(1) pi-stacked hydrophobic, (4) C-H bonds.
INH09	-7.7	O2-Thy8, O2-Thy4, N3-Ade5	(2) Conventional H bond. (1) unfavorable acceptor-acceptor.
INH10	-8.3	O2-Thy6(A), O2-Thy6(B), O4-Thy6(B), C4-Ade5, O4-Ade7	(3) Conventional H bond, (2) C-H bonds.
INH11	-8.8	O4-Thy6, N3-Ade5, O4-Ade7, C5-Thy8, O4-Ade5, Phenylring-Ade7, Phenylring-Ade5	(3) Conventional H bond, (2) C-H bonds. (2) pi-alkyl hydrophobic.
INH12	-8.4	O4-Ade7(A), O2-Thy6, O4-Ade7(B)	(2) Conventional H bond, (1) C-H bonds.
INH13	-6.5	N3-Ade5, Phenylring-Thy4	(2) C-H bonds. (2) pi- pi stacked hydrophobic.
INH14	-9.2	O4-Ade7, O2-Thy6, O4-Ade5, Op1-Thy8	(2) Conventional H bond, (1) C-H bonds. (1) pi- anion electrostatic.
INH15	-6.9	O2-Thym8, O2-Thy4, C4-Thy8, C4-Ade9, O2-Thy4	(2) Conventional H bond, (1) C-H bonds. (1) pi-sigma hydrophobic
INH16	-6.8	O2-Thy6, O2-Thy6	(2) C-H bonds.
INH17	-7.7	O2-Thy8, O2-Thy4, O2-Thy4, O4-Ade5, OP1-Thy6	(2) Conventional H bond, (2) C-H bonds. (1) pi-anion electrostatic bond.
INH18	-6.9	O2-Thy4, O2-Thy8, O4-Ade5, N3-Ade9, O3-Ade9, O2-Thy8	(3) Conventional H bond, (3) C-H bonds.
INH19	-8.8	O4-Ade7, O4-Ade7, O2-Thy6	(1) Conventional H bond, (2) C-H bonds.
INH	-5.6	O2-Thy4, O2-Thy4, O4-Ade5, O2-Thy8	(4) Conventional H bond.
PT	-6.5	N6-Ade5(A), N6-Ade5(B), N6-Ade3, C6-Thy4, C7-Ade6(A), C7-Ade(B), N6-Ade7(B), N6-Ade3(A)	(4) Conventional H bond, (1) C-H bonds. (1) pi- sigma hydrophobic. (1) unfavorable donor-donor.

Abbreviations: The table includes several key abbreviations to represent various atoms and molecular components relevant to DNA structure. "O" stands for an oxygen atom, "H" denotes a hydrogen atom, "N" refers to a nitrogen atom, "Op" specifically represents an oxygen atom within a phosphate group, and "C" is used for a carbon atom. The nucleobases are also abbreviated, with "Cyt" representing cytosine, "Ade" for adenine, "Thy" for thymine, and "Gua" for guanine, all of which are essential components of DNA.

Table 4L: Modeling Data of the Reported Compounds on DNA Fragment 1MTG.

Codes	ΔG	DNA Residues Involved in Interaction	Number & type of bonds Involved in Interaction
INH01	-5.6	Phenylring-Ade8, O4-Thym5, O2-Cyt4	(1) Conventional H bond, (1) C-H bonds, (1) Pi-Pi T-shaped hydrophobic.
INH02	-5.9	O4-Thym11, O2-Thym11, O4-Cyt12	(4) Conventional H bond, (1) C-H bonds.
INH03	-6.6	H22-Gua9, O4-Thym11, O2-Cyt10, O2-Thym11, H2-Ade2, H1-Gua3.	(1) Conventional H bond, (2) C-H bonds.
INH04	-5.7	O4-Thym5, H2-Ade8, H1-Thym11, Phenylring-Thym11	(2) Conventional H bond, (2) C-H bonds, (1) pi-alkyl hydrophobic.
INH05	-6.4	O4-Thym5, O2-Thym11, H22-Gua3	(4) C-H bonds.
INH06	-6.5	O2-Cyt4, O4-Thym5, H22-Gua3, Phenylring-Gua3, Phenylring-Cyt4, O2-Cyt10.	(3) Conventional H bond, (2) pi-alkyl hydrophobic, (1) unfavorable acceptor-acceptor.
INH07	-6.3	O4-Thym5, O2-Cyt4, Phenylring-Ade8, Phenylring-Gua9, O2-Thym11, Phenylring-Gua3.	(2) Conventional H bond, (2) pi-pi stacked hydrophobic, (1) C-H bonds, (1) pi-alkyl hydrophobic.
INH08	-5.9	O4-Thym5, H2-Ade8, O2-Thym11, Phenylring-Thym11.	(2) Conventional H bond, (2) C-H bonds, (1) pi-alkyl hydrophobic.

INH09	-6.7	O2-Thym11, Phenylring-Gua3, Phenylring-Cyt4, Phenylring-Gua3, 5ring-Gua3, Phenylring-Thym5, O4-Thym5.	(1) Conventional H bond, (5) Pi-Pi stacked hydrophobic, (1) unfavorable acceptor-acceptor.
INH10	-6.5	H22-Gua3, H21-Gua3, H22-Gua9, H22-Gua9, H1-Ade2, H4-Cyt4, Phenylring-Ade2, Phenylring-Cyt4.	(4) Conventional H bond, (2) C-H bonds, (1) Pi-Pi T-shaped hydrophobic, (1) pi-alkyl hydrophobic.
INH11	-6.3	H22-Gua9, H23-Gua9, H22-Gua3, H1-Gua3, Phenylring-Gua3.	(3) Conventional H bond, (1) C-H bonds. (1) Pi-Pi T-shaped hydrophobic.
INH12	-6.1	H22-Gua3, H21-Gua9, H22-Gua9, H22-Gua1, Phenylring-Gua3, Phenylring-Gua2.	(4) Conventional H bond, (1) Pi-Pi T-shaped hydrophobic.
INH13	-5.4	O4-Thym5, H22-Gua9, Phenylring-Gua9, 5ring-Gua9, Phenylring-Cyt4	(4) Conventional H bond. (1) Pi-Pi T-shaped hydrophobic.
INH14	-6.5	O4-Thym5, O2-Cyt4, H22-Gua3	(2) Conventional H bond, (1) Pi-donor H bonds.
INH15	-5.7	O2-Cyt4, O2-Thym11, H4-Thym11, Phenylring-Ade2, Phenylring-Ade2.	(2) Conventional H bond, (1) C-H bonds. (1) Pi-Pi T-shaped hydrophobic, (1) pi-alkyl hydrophobic.
INH16	-5.2	O4-Thym5, O4-Thym5, O4-Gua9, Phenylring-Gua9, Phenylring-Ade8, Phenylring-Gua9	(2) Conventional H bond, (2) Pi-Pi T-shaped hydrophobic, (1) pi-stacked hydrophobic, (1) C-H bonds.
INH17	-6.2	O2-Cyt4, O2-Thym11, H22-Gua3, H4-Thym11, H1-Cyt4	(3) Conventional H bond, (1) Pi-Pi T-shaped hydrophobic, (2) C-H bonds.
INH18	-6.0	H21-Gua9, O2-Cyt4	(2) Conventional H bond.
INH19	-6.5	H22-Gua9, O2-Cyt10, O4-Thym11, O2-Thym11	(4) Conventional H bond.
INH	-4.6	O4-Thym5, O2-Cyt4, O4-Thym5	(3) Conventional H bond.
PT	-6.9	H42-Cyt10, O6-Gua3, H41-Cyt4, H42-Cyt4, H3-Gua1, Op2-Gua9, Op2-Gua3, N7-Gua3	(4) Conventional H bond, (2) C-H bonds, (2) pi-anion electrostatic, (1) unfavorable acceptor-acceptor.

Abbreviations: The table includes several key abbreviations to represent various atoms and molecular components relevant to DNA structure. "O" stands for an oxygen atom, "H" denotes a hydrogen atom, "N" refers to a nitrogen atom, "Op" specifically represents an oxygen atom within a phosphate group, and "C" is used for a carbon atom. The nucleobases are also abbreviated, with "Cyt" representing cytosine, "Ade" for adenine, "Thy" for thymine, and "Gua" for guanine, all of which are essential components of DNA.

Table 2M: Modeling Data of the Reported Compounds on DNA Fragment 1Z3F.

Codes	ΔG	DNA Residues Involved in Interaction	Number & type of bonds Involved in Interaction
INH01	-5.9	O2-Cyt5, N2-Gua2, Phenylring-Gua6, 5ring-Gua6, Phenylring-Cyt1, Phenylring-Gua2, 5ring-Gua2.	(1) Conventional H bond, (1) Pi-donor H bonds, (6) Pi-Pi stacked hydrophobic.
INH02	-6.0	O2-Cyt5, N2-Gua2, Phenylring-Gua6, 5ring-Gua6, Phenylring-Gua2, 5ring-Gua2, Phenylring-Cyt5.	(1) Conventional H bond, (1) Pi-donor H bonds, (5) Pi-Pi stacked hydrophobic.
INH03	-6.4	O2-Thym4, N2-Gua2	(2) Conventional H bond.
INH04	-5.4	N2-Gua2, O2-Thym4, O2-Cyt5, O4-Cyt5	(4) Conventional H bond, (1) pi-alkyl hydrophobic.
INH05	-6.0	N2-Gua2, N3-Gua2, Phenylring-Gua2, 5ring-Gua2, Phenylring-Cyt1, Phenylring-Gua6, 5ring-Gua6, Phenylring-Cyt5, N2-Gua6.	(2) Conventional H bond, (1) Pi-donor H bonds, (1) pi-sigma hydrophobic, (3) Pi-Pi stacked hydrophobic.
INH06	-6.4	N2-Gua2, Phenylring-Gua2, Phenylring-Gua6, 5ring-Gua6, Phenylring-Ade5, 5ring-Cyt5.	(1) Pi-donor H bonds, (1) pi-sigma hydrophobic, (3) Pi-Pi stacked hydrophobic.
INH07	-5.6	N2-Gua2, O2-Thym4, O2-Cyt5, C2-Ade3, N3-Ade3, O2-Cyt5, Phenylring-Ade3, Phenylring-Thym4.	(4) Conventional H bond, (3) C-H bonds, (1) Pi-Pi T-shaped hydrophobic.
INH08	-5.8	N2-Gua2, N2-Gua6, Phenylring-Gua2, 5ring-Gua2, Phenylring-Gua6, 5ring-Gua6, Phenylring-Cyt1, Phenylring-Gua6, Phenylring-Cyt5, Phenylring-Gua2.	(2) Pi-donor H bonds, (4) Pi-Pi stacked hydrophobic.

INH09	-7.2	O4-Thym4, O2-Cyt5, O4-Ade3, O4-Gua6, N2-Gua2, N2-Gua6, Phenylring-Ade3, Phenylring-Gua2, 5ring-Gua2, Phenylring-Gua6, 5ring-Gua6, 5ring-Gua2, Phenylring-Cyt5.	(2) Conventional H bond, (2) C-H bonds, (1) unfavorable acceptor-acceptor.
INH10	-6.1	O2-Thym4, N2-Gua2	(3) Conventional H bond, (2) C-H bonds, (4) Pi-Pi stacked hydrophobic, (10) Pi-Pi T-shaped hydrophobic.
INH11	-6.1	O4-Gua2, N7-Gua6, Phenylring-Gua6, 5ring-Gua2, Phenylring-Cyt1.	(2) Conventional H bond.
INH12	-6.1	O2-Thym4, N2-Gua2	(2) Conventional H bond, (3) Pi-Pi stacked hydrophobic, (1) Pi-Pi T-shaped hydrophobic.
INH13	-5.3	O2-Cyt5, O2-Thym4, O4-Cyt5, C1-Thym1, N2-Gua2	(2) Conventional H bond.
INH14	-6.5	O2-Thym4(A), O2-Thym(B), N2-Gua2, N3-Gua2, C1-Thym4, O4-Gua6, O2-Cyt5.	(2) Conventional H bond, (3) C-H bonds, (2) Pi-donor H bonds.
INH15	-5.8	O4-Cyt5, O2-Thym4, N2-Gua2, C5-Cyt5	(2) Conventional H bonds, (1) Pi-donor H bonds, (1) C-H bonds.
INH16	-5.0	O2-Cyt5, O2-Thym9, O2-Thym4, O4-Cyt5	(2) Conventional H bond, (2) C-H bonds, (4) Pi-Pi stacked hydrophobic,
INH17	-6.6	N3-Ade3, O2-Cyt5, N2-Gua2, N2-Gua6, N2-Gua2, O4-Gua6, Phenylring-Gua6, 5ring-Gua6, Phenylring-Gua2, 5ring-Gua2, Phenyl-Cyt1, Phenyl-Cyt5.	(4) Conventional H bond, (1) C-H bonds, (1) Pi-donor H bonds, (1) unfavorable donor-donor.
INH18	-6.0	N2-Gua2, N3-Gua2, O4-Gua2, Phenylring-Gua6, 5ring-Gua6, Phenylring-Gua2, 5ring-Gua2, Phenylring-Cyt5, Phenylring-Cyt1.	(3) Conventional H bond, (6) Pi-Pi stacked hydrophobic.
INH19	-6.5	O4-Thym4, N2-Gua2.	(1) Conventional H bond, (1) Pi-donor H bonds.
INH	-5.0	O4-Gua2, N2-Gua6, Phenylring-Gua2, 5ring-Gua2, Phenylring-Gua6, Phenylring-Cyt1.	(1) Conventional H bond, (4) Pi-Pi stacked hydrophobic, (1) Pi-donor H bonds, (1) C-H bonds.
PT	-7.8	O2-Thym4, O2-Cyt5, N2-Gua2.	(5) Conventional H bond, (10) Pi-Pi T-shaped hydrophobic.

Abbreviations: The table includes several key abbreviations to represent various atoms and molecular components relevant to DNA structure. "O" stands for an oxygen atom, "H" denotes a hydrogen atom, "N" refers to a nitrogen atom, "Op" specifically represents an oxygen atom within a phosphate group, and "C" is used for a carbon atom. The nucleobases are also abbreviated, with "Cyt" representing cytosine, "Ade" for adenine, "Thy" for thymine, and "Gua" for guanine, all of which are essential components of DNA.

Table 2N: Modeling Data of the Reported Compounds on DNA Fragment 1D32.

Codes	ΔG	DNA Residues involved in Interaction (1D32)	Number & type of bonds Involved in Interaction
INH01	-6.3	N4-Gua4, phenylring-Gua6, 5ring-Gua6, phenylring-Cyt5, phenylring-Cyt4, 5ring-Cyt4, phenylring-Cyt3	(6) Pi-Pi stacked hydrophobic. (1) Pi-donor H bonds.
INH02	-6.6	O4-Gua, O2-Cyte7, N2-Gua2	(3) Conventional H bond, (1) Pi-Pi T-shaped hydrophobic, (3) Pi-stacked hydrophobic.
INH03	-6.9	N2-Gua4, phenylring-Cyt3, phenylring-Cyt5, phenylring-Gua4, phenylring-Gua6, 5ring-Cyt4	(1) Conventional H bond. (5) Pi-Pi stacked hydrophobic.
INH04	-6.8	O2-Cyt3, O4-Gua4, N3-Gua4, N1-Gua6	(5) Conventional H bond, (1) Pi-donor H bonds, (4) Pi-Pi stacked hydrophobic, (1) Pi-Pi T-shaped hydrophobic.
INH05	-6.0	O4-Gua6, O2-Cyt3, O4-Gua4, N2-Gua2	(4) Conventional H bond, (1) Pi-donor H bonds, (2) Pi-Pi stacked hydrophobic.
INH06	-6.5	O4-Gua4, N2-Gua2, O4-Gua6.	(3) Conventional H bond, (1) C-H bonds. (1) pi-alkyl hydrophobic.
INH07	-6.6	O4-Gua6, O2-Cyt3, O4-Gua4, phenylring-Gua6, 5ring-Gua6, phenylring-Gua4, phenylring-Cyt5.	(3) Conventional H bond, (4) Pi-Pi stacked hydrophobic, (1) Pi-donor H bonds.
INH08	-5.5	O4-Gua4, N2-Gua2, Phenylring-Gua2	(2) Conventional H bond, (1) pi-alkyl hydrophobic.

INH09	-7.4	O2-Cyt7, O4-Gua8, Phenylring-Gua8, 5ring-Gua8, Phenylring-Cyt7, Phenylring-Gua2, N2-Gua2	(2) Conventional H bond, (6) Pi-Pi stacked hydrophobic, (1) Pi-donor H bonds.
INH10	-6.4	N1-Gua6, O4-Gua4, N2-Gua6, Phenylring-Gua6, 5ring-Gua6, Phenylring-Gua4, 5ring-Gua4, Phenylring-Cyt3	(1) Conventional H bond, (2) C-H bonds. (1) Pi-donor H bonds, (1) Pi-sigma hydrophobic.
INH11	-6.3	Phenylring-Gua4, 5ring-Gua4, Phenylring-Cyt3	(3) Pi-Pi stacked hydrophobic.
INH12	-6.4	O2-Cyt7, N2-Gua6, Phenylring-Gua4, 5ring-Gua4, Phenylring-Gua6, 5ring-Gua6, Phenylring-Cyt5.	(2) Conventional H bond, (5) pi- pi stacked hydrophobic, (1) unfavorable donor-donor, (2) C-H bonds, (1) Pi-donor H bonds.
INH13	-5.3	O4-Cyt7, O2-Cyt5, O4-Gua6.	(3) C-H bonds, (5) pi- pi stacked hydrophobic, (1) unfavorable donor-donor.
INH14	-6.9	O4-Gua8, 5ring-Gua8, Phenylring-Gua8, 5ring-Gua8, Phenylring-Cyt7.	(1) Conventional H bond, (1) Pi-sigma hydrophobic, (5) Pi-Pi stacked hydrophobic.
INH15	-6.7	O4-Gua2, O4-Gua8, N2-Gua2, Phenylring-Gua8, 5ring-Gua8, Phenylring-Gua2, Phenylring-Cyt7.	(2) Conventional H bond, (3) Pi-stacked hydrophobic, (1) Pi-donor H bonds.
INH16	-5.7	O4-Gua8, N2-Gua2, Phenylring-Gua8, 5ring-Gua8, Phenylring-Cyt7.	(1) Conventional H bond, (3) Pi-Pi stacked hydrophobic, (1) Pi-donor H bonds.
INH17	-6.7	O4-Gua4, N2-Gua4, O2-Cyt7, N2-Gua6, Phenylring-Gua4, 5ring-Gua4, Phenylring-Gua6, 5ring-Gua6, Phenylring-Cyt7	(2) Conventional H bond, (5) pi- pi stacked hydrophobic, (3) C-H bonds, (1) unfavorable donor-donor.
INH18	-6.3	O4-Gua8, O2-Cyt7, N2-Gua2, Phenylring-Gua2, Phenylring-Gua8, 5ring-Gua8, Phenylring-Cyt7	(1) Conventional H bond, (4) pi- pi stacked hydrophobic, (1) Pi-Pi T-shaped hydrophobic, (1) C-H bonds, (1) Pi-donor H bonds.
INH19	-6.8	N2-Gua4, , Phenylring-Gua6, 5ring-Gua6, Phenylring-Gua4, 5ring-Gua4, Phenylring-Cyt3	(1) Pi-donor H bonds, (6) Pi-Pi stacked hydrophobic.
INH	-5.4	O4-Gua6, O4-Gua4, O5-Gua4, N1-Gua6, Phenylring-Gua6, 5ring-Gua6, Phenylring-Gua6, Phenylring-Gua4	(5) Conventional H bond, (4) pi- pi stacked hydrophobic, (1) Pi-donor H bonds.
PT	-8.6	N2-Gua2, O2-Cyt7, O2-Cyt3, O4-Gua8, N2-Gua2, N2-Gua6, N2-Gua4, N3-Gua2, Phenylring-Cyt3, Phenylring-Gua6, 5ring-Gua6, Phenylring-Gua4, 5ring-Gua4.	(4) Conventional H bond, (5) pi- pi stacked hydrophobic, (1) C-H bonds, (1) Pi-donor H bonds, (2) unfavorable donor-donor, (1) unfavorable acceptor-acceptor.

Abbreviations: The table includes several key abbreviations to represent various atoms and molecular components relevant to DNA structure. "O" stands for an oxygen atom, "H" denotes a hydrogen atom, "N" refers to a nitrogen atom, "Op" specifically represents an oxygen atom within a phosphate group, and "C" is used for a carbon atom. The nucleobases are also abbreviated, with "Cyt" representing cytosine, "Ade" for adenine, "Thy" for thymine, and "Gua" for guanine, all of which are essential components of DNA.

Table 20: Modeling Data of the Reported Compounds on DNA Fragment 1ZNA.

Codes	ΔG	DNA Residues Involved in Interaction	Number & type of bonds Involved in Interaction
INH01	-5.7	O2-Cyt5, OP2-Gua8, N2-Gua6, N2-Gua2	(2) Conventional H bond, (2) Pi-donor H bonds.
INH02	-6.3	N2-Gua2, OP2-Gua4, O3-Cyt3, O2-Cyt3, O3-Cyt5, N2-Gua6.	(5) Conventional H bond, (1) pi- anion electrostatic.
INH03	-6.7	Op2-Gua2, O2-Cyt7, O3-Cyt7, N2-Gua4, O3-Cyt1, Op2-Gua4, O2-Cyt3, O2-Cyt1, N2-Gua2.	(5) Conventional H bond, (1) pi- anion electrostatic, (1) Pi-donor H bonds, (2) C-H bonds
INH04	-6.2	O3-Cyt7, N2-Gua8, Op2-Gua2, Op1-Gua8, O3-Cyt3, O2-Cyt3, O3-Cyt1.	(3) Conventional H bond, (3) C-H bonds bonds, (1) pi- anion electrostatic.
INH05	-6.3	OP2-Gua2, N2-Gua8, O3-Cyt7, O3-Cyt1, O2-Cyt3, O3-Cyt5, O3-Cyt3.	(3) Conventional H bond, (3) C-H bonds.

INH06	-6.2	OP2-Gua2, N2-Gua8, O3-Cyt7, Op1-Gua8, O3-Cyt1, O3-Cyt5, O2-Cyt3, O3-Cyt3, Op2-Gua6.	(3) Conventional H bond, (4) C-H bonds. (1) pi- anion electrostatic.
INH07	-6.1	Op2-Gua2, N2-Gua8, O3-Cyt7, Op1-Gua8, N2-Gua2, O3-Cyt3, O2-Cyt3.	(3) Conventional H bond, (1) pi- anion electrostatic, (4) C-H bonds, (1) Pi-donor H bonds.
INH08	-5.9	O3-Cyt1, N2-Gua8, Op2-Gua8, N2-Gua6, Op2-Gua4, Op2-Gua8.	(4) Conventional H bond, (2) pi- anion electrostatic, (1) C-H bonds.
INH09	-6.5	N2-Gua6, Op2-Gua4, O2-Cyt3, O3-Cyt3, O2-Cyt7, Op2-Gua8, Op1-Gua4, Op1-Gua4.	(6) Conventional H bond, (2) pi- anion electrostatic.
INH10	-6.7	O3-Cyt3, O2-Cyt7, N2-Gua8, N2-Gua2, N2-Gua4.	(4) Conventional H bond, (1) Pi-donor H bonds.
INH11	-6.8	Op2-Gua2, O2-Cyt3, O2-Cyt7, O2-Cyt3, O3-Cyt1, Op2-Gua4, O3-Cyt3, N2-Gua6, N2-Gua2.	(4) Conventional H bond, (3) C-H bonds, (1) Pi-donor H bonds, (2) unfavorable donor-donor,
INH12	-6.7	N2-Gua6, O3-Cyt3, O2-Cyt3, N2-Gua8, N2-Gua2, Op2-Gua2, N2-Gua2	(4) Conventional H bond, (2) C-H bonds, (1) Pi-donor H bonds.
INH13	-6.3	Op2-Gua2, N2-Gua8, O3-Cyt7, N2-Gua6, O3-Cyt1, C1-Cyt7, O2-Cyt3, O3-Cyt3, Op2-Gua4	(4) Conventional H bond, (3) C-H bonds.
INH14	-7.1	N2-Gua6, O3-Cyt3, O2-Cyt3, O2-Cyt7, N2-Gua4, Op2-Gua4, O2-Cyt1.	(4) Conventional H bond, (1) Pi-donor H bonds.
INH15	-5.9	O2-Cyt3, O3-Cyt3, Op2-Gua4, O2-Cyt7, Op1-Gua8, Op2-Gua8.	(3) Conventional H bond, (1) C-H bonds, (2) pi- anion electrostatic.
INH16	-5.8	Op2-Gua2, O3-Cyt7, N2-Gua8, Op1-Gua8, O3-Cyt1, O2-Cyt3, O3-Cyt3.	(3) Conventional H bond, (2) C-H bonds, (1) pi- anion electrostatic.
INH17	-6.3	N2-Gua6, O2-Cyt3, Op2-Gua4, O3-Cyt3, N2-Gua2, N2-Gua8, Op1-Gua8, Op1-Gua4, Op2-Gua8.	(6) Conventional H bond, (1) pi- anion electrostatic.
INH18	-6.1	N2-Gua6, O2-Cyt7, O2-Cyt3, O3-Cyt3, Op1-Gua4, N2-Gua4, Op2-Gua4	(4) Conventional H bond, (2) C-H bonds, (1) Pi-donor H bonds, (2) pi- anion electrostatic.
INH19	-6.8	O2-Cyt3, O2-Cyt7, O3-Cyt3, N2-Gua4.	(3) Conventional H bond, (1) C-H bonds, (1) Pi-donor H bonds.
INH	-4.7	O3-Cyt5, Op2-Gua6, O2-Cyt3, O3-Cyt3, Op2-Gua4, O2-Cyt5, N2-Gua6.	(4) Conventional H bond, (1) C-H bonds, (1) Pi-donor H bonds.
PT	-6.6	O2-Cyt7, N2-Gua6, Op1-Gua8, C5-Gua6, O3-Cyt7, Op2-Gua8, Op2-Cyt7, N2-Gua2.	(3) Conventional H bond, (2) C-H bonds, (2) pi- anion electrostatic, (1) Pi-donor H bonds, (1) unfavorable donor-donor.

Abbreviations: The table includes several key abbreviations to represent various atoms and molecular components relevant to DNA structure. "O" stands for an oxygen atom, "H" denotes a hydrogen atom, "N" refers to a nitrogen atom, "Op" specifically represents an oxygen atom within a phosphate group, and "C" is used for a carbon atom. The nucleobases are also abbreviated, with "Cyt" representing cytosine, "Ade" for adenine, "Thy" for thymine, and "Gua" for guanine, all of which are essential components of DNA.

Copyright: © 2025 Abdul M Gbaj. This Open Access Article is licensed under a [Creative Commons Attribution 4.0 International \(CC BY 4.0\)](#), which permits unrestricted use, distribution, and reproduction in any medium, provided the original author and source are credited.